Reliability of SM2RAIN precipitation datasets in comparison to gauge observations and hydrological modelling over arid regions

Frédéric Satgé, Yawar Hussain, Jorge Molina-carpio, Ramiro Pillco, Coralie Laugner, Gulraiz Akhter, Marie-paule Bonnet

Received: 20 December 2019 | Revised: 24 April 2020 | Accepted: 8 June 2020

DOI: 10.1002/joc.6704

International Journal of Climatology RMetS

RESEARCH ARTICLE

Reliability of SM2RAIN precipitation datasets in comparison to gauge observations and hydrological modelling over arid regions

Frédéric Satgé[1] | **Yawar Hussain**[2] | **Jorge Molina-Carpio**[3] | **Ramiro Pillco**[3] | **Coralie Laugner**[1] | **Gulraiz Akhter**[4] | **Marie-Paule Bonnet**[1]

[1]UMR228 ESPACE-DEV, Université de Montpellier, IRD, Université des Antilles, Université de Guyane, Université de La Réunion, Montpellier, France

[2]Environmental Engineering and Earth Science Department, Clemson University, Clemson, South Carolina, USA

[3]Universidad Mayor de San Andres (UMSA), Instituto de Hidráulica e Hidrologia (IHH), La Paz, Bolivia

[4]Department of Earth Science, Quaid-i-Azam University, Islamabad, Pakistan

Correspondence
Frédéric Satgé, UMR228 ESPACE-DEV, Université de Montpellier, IRD, Université des Antilles, Université de Guyane, Université de La Réunion, Montpellier, France, 500 rue Jean-François Breton, Montpellier 34000, France.
Email: frederic.satge@ird.fr

Abstract

Numerous satellite-based precipitation datasets have been successively made available. Their precipitation estimates rely on clouds properties derived from microwave and thermal sensors in a so-named 'top-down' approach. Recently, a 'bottom-up' approach to infer precipitation from soil moisture (SM) estimates has resulted in the release of two new precipitation datasets (P-datasets). One uses satellite-based SM estimates from the European Spatial Agency (ESA) Climate Change Initiative (CCI) (SM2RAIN-CCI) while the other uses satellite-based SM from European Organization for the Exploitation of Meteorological Satellites (EUMETSAT) Advanced SCATterometer (ASCAT) (SM2RAIN-ASCAT). This study assesses SM2RAIN-ASCAT and -CCI reliability over two arid regions: Bolivian and Peruvian Altiplano and Pakistan (South Asia) using (a) direct comparisons with rain gauges and (b) testing the sensitivity of streamflow modelling to the P-datasets. Selecting two different regions and different indicators helps to assess whether the P-dataset reliability varies depending on the assessment method and location. For comparison purposes, the most reliable P-datasets from the literature are also considered (IMERG-E v.6, IMERG-L v.6, IMERG-F v.6, CHIRPS v.2 and MSWEP v.2.2). Compared to rain gauge observations and based on the modified Kling–Gupta Efficiency (KGE) values, the SM2RAIN-ASCAT and -CCI are more accurate in the Altiplano than in Pakistan. This difference is explained by a more favourable physical context for satellite-based SM estimates in the Altiplano. Over the Altiplano and despite an overall positive bias, SM2RAIN-ASCAT describes rain gauges temporal dynamics as well as IMERG-F v.6, CHIRPS v.2 and MSWEP v.2.2 and provides streamflow simulations very close to those obtained when using IMERG-F v.6, CHIRPS v.2 and MSWEP v.2.2 as forcing data.

KEYWORDS

arid region, assessment, gauges, hydrological modelling, satellite precipitation, SM2RAIN

1 | INTRODUCTION

1.1 | Precipitation monitoring challenge across remote regions

Precipitation is a key component of the water cycle, which is under unprecedented pressures due to the combined effects of population growth and climate change. Precipitation estimates are therefore essential to adapt and for anticipating ongoing changes. However, precipitation is generally collected from sparse and unevenly distributed gauge networks, which are subject to large uncertainties, especially in remote regions. Additionally, most of the rain gauge data are still collected manually, so the collection and digitization of these data are subject to human error and are a source of delay in data availability. Data collection in trans-boundary basins is an even more complex task due to potential conflicts related to water use. In these difficult circumstances, satellite-based precipitation products (SPPs), with a near-global spatial coverage and free online availability, are a potentially very effective alternative.

1.2 | Opportunities and limitations of available SPPs

Several SPPs have been made available in recent decades to provide precipitation estimates on regular grids and over a continuous time scale. The first generation of SPPs emerged in 1997 when the Tropical Rainfall Measuring Mission (TRMM) was jointly launched by the National Aeronautics and Space Administration (NASA) and the Japan Aerospace Exploration Agency (JAXA). Over the past 18 years, the TRMM Multisatellite Precipitation Analysis (TMPA) (Huffman *et al*., 2007), the Climate Prediction Centre MORPHing (CMORPH) (Joyce *et al*., 2004), the Precipitation Estimation from Remotely Sensed Information using Artificial Neural Networks (PERSIANN) (Sorooshian *et al*., 2000) and the Global Satellite Mapping Precipitation (GSMaP) Kubota et al., 2007 SPPs have been developed on the basis of the TRMM mission. In 2014, the Global Precipitation Measurement (GPM) mission was launched to ensure the continuity of the TRMM mission. The launch of the GPM mission gave rise to the second generation of SPPs, which includes the Integrated Multi-SatellitE Retrievals for GPM (IMERG) (Huffman et al., 2019b) and a new version of GSMaP (Yamamoto and Shige, 2014).

At the same time, some works have explored previous SPPs and missions to improve precipitation estimates and widen time windows: the generation of long-term SPP. This is the case of the PERSIANN-Climate Data Record (PERSIANN-CDR) (Ashouri *et al*., 2015), the Multi-Source Weighted-Ensemble Precipitation (MSWEP) (Beck *et al*., 2018) and the Climate Hazards Group Infra-Red Precipitation with Station data (CHIRPS) (Funk *et al*., 2015).

The first, second and long-term SPPs have shortcomings because precipitation estimates are inferred from cloud properties retrieved from Passive Micro Waves (PMWs) and/or Infra-Red (IR) observations using a so-called 'top-down' approach. The PMWs-based precipitation estimates are difficult in areas where significant land cover variability leads to changes in emissivity and/or temperature, which can produce background signals quite similar to those generated by precipitation (see for example, Ferraro *et al*., 1998; Levizzani *et al*., 2002; Tian and Peters-Lidard, 2007). For instance, frozen areas appear similar to upper ice precipitation in the scattering signal resulting in an overestimate of precipitation (e.g., Mourre *et al*., 2016). Additionally, PMWs sensors are on board Low Earth Orbital (LEO) satellites with irregular sampling and limited passage that prevent the correct capture of short-term and slight precipitation events (Tian *et al*., 2009; Gebregiorgis and Hossain, 2013). This feature introduces errors in precipitation estimates over arid regions and/or during the dry season (e.g., Shen *et al*., 2010; Prakash *et al*., 2014; Satgé *et al*., 2016). IR sensors have difficulties detecting precipitation events based on warm cloud because the temperature threshold used to separate rainy clouds from others may be too low (e.g., Dinku *et al*., 2007, 2010; Hirpa *et al*., 2010; Gebregiorgis and Hossain, 2013). This characteristic introduces errors in precipitation estimates over mountainous regions (Hussain et al., 2017; Satgé et al., 2017a). In this context, the reliability of the SPPs based on the 'top-down' approach is expected to vary spatially depending on the occurrence of the aforementioned factors (i.e., emissivity/temperature contrast, arid context, mountains).

1.3 | Novel approach for precipitation estimates based on soil moisture measurements

Recently, the Soil Moisture (SM) to Rain (SM2RAIN) algorithm (Brocca *et al*., 2013) was developed to deduce precipitation estimates from SM measurements in a so-called 'bottom-up' approach. The SM2RAIN algorithm has been successfully applied to retrieve precipitation estimates from (a) in situ SM measurements (Brocca *et al*., 2013, 2015) and (b) satellite-based SM estimates as the Soil Moisture Ocean Salinity Mission (SMOS) (Brocca *et al*., 2014, 2016; Tarpanelli *et al*., 2017), the Advanced Microwave Scanning Radiometer (AMSR) (Brocca *et*

al., 2014; Tarpanelli *et al*., 2017), the Soil Moisture Active and Passive (SMAP) (Koster *et al*., 2016; Tarpanelli *et al*., 2017), the Advanced SCATterometer (ASCAT) (Brocca *et al*., 2014; Ciabatta *et al*., 2015, 2017; Massari *et al*., 2017; Tarpanelli *et al*., 2017).

The use of satellite-based SM estimates is of particular interest to overcome the limitations of the 'top-down' approach used for the estimation of the clouds´ properties. Furthermore, as a signature of accumulated precipitation up to the time of satellite observation, the use of SM measurements can mitigate the snapshot of the sensors onboard LEO satellites (Ciabatta *et al*., 2018; Brocca *et al*., 2019). In this context, the SM2RAIN algorithm was used to release two precipitation datasets (P-datasets). The first uses SM estimates from the European Spatial Agency (ESA) Climate Change Initiative (CCI) dataset (Ciabatta *et al*., 2018) (hereafter SM2RAIN-CCI) and the second uses SM estimates from the European Organization for the Exploitation of Meteorological Satellites (EUMETSAT) Advanced SCATterometer (ASCAT) dataset (Brocca *et al*., 2019) (here after SM2RAIN-ASCAT).

Despite the interest of the product developers (Brocca *et al*., 2019), the SM2RAIN P-datasets reliability has only been systematically reported in India (Prakash, 2019), Brazil (Paredes-Trejo *et al*., 2019; Souto *et al*., 2019), Pakistan (Rahman *et al*., 2019), West Africa (Satgé *et al*., 2020), Austria (Sharifi *et al*., 2019) and China (Zhang *et al*., 2019). These studies used precipitation gauge observations as a reference to assess the potential benefits of the SM2RAIN P-datasets ('bottom-up' approach) compared to well-established state-of-the art SPPs. These studies concluded that the relative performances of the SM2RAIN P-datasets vary from region to region.

For instance, some studies show that previously released SPPs are more reliable than SM2RAIN P-datasets over specific regions. SM2RAIN-CCI monthly estimates have a significant bias over India (Prakash, 2019) and West Africa (Satgé *et al*., 2020) and in these studies CHIRPS v.2 and MSWEP v.2.2 were more reliable. Over Austria, MSWEP v.2.2 shows stronger agreement with gauge observations than SM2RAIN-ASCAT at daily and monthly time steps (Sharifi *et al*., 2019). TMPA v.7 provides more reliable daily precipitation estimates than SM2RAIN-ASCAT and -CCI in Pakistan (Rahman *et al*., 2019). On the contrary, other studies show that SM2RAIN P-datasets are more reliable than the previously released SPPs. For example, both SM2RAIN-ASCAT and -CCI have performed as well as or better than TMPA v.7 over different Brazilian regions (Paredes-Trejo *et al*., 2019). Similarly, SM2RAIN-ASCAT daily precipitation estimates are more reliable than IMERG daily precipitation estimates in the southern hemisphere (Brocca *et al*., 2019) and so are monthly precipitation estimates over China (Zhang *et al*., 2019). It is worth mentioning that the divergent results reported in the above-mentioned studies may be due to the different methodological approaches adopted such as the preprocessing P-dataset, the statistical metrics and the time periods considered.

1.4 | Objectives

In accordance with the previously established state of the art, this study evaluates the reliability of SM2RAIN-ASCAT and -CCI over two arid regions, (a) the South American Andean Plateau (hereafter called Altiplano) and (b) Pakistan. Our objective is to assess the reliability of SM2RAIN P-datasets in space without any potential influence of the methodological steps used. The assessment of reliability comprises two indicators: (a) gauge observations and (b) streamflow simulation using sensitivity analysis of a lumped hydrological model in different basins. The purpose of using different indicators was to assess their influence on the P-dataset reliability.

IMERG (-Early, -Late and -Final), MSWEP v.2.2 and CHIRPS v.2 P-datasets for a common period of data availability were used to assess the potential improvement of SM2RAIN P-datasets over the most efficient and currently available SPPs over the considered regions (Satgé *et al*., 2017b; Satgé *et al*., 2019a; Satgé *et al*., 2019b). It is also an opportunity to assess the potential benefits of the 'bottom-up' (SM2RAIN-CCI and -ASCAT) compared to the 'top-down' approach using gauge-based (CHIRPS, MSWEP and IMERG-Final) or satellite-only (IMERG-Early and -Late) products.

2 | MATERIALS AND METHODS

2.1 | Study area

Two arid regions are considered in this study. The first one, the Altiplano, is located southward of the equator and covers an area of about 192,390 km^2. The Altiplano is an endorheic system situated at 4000 m.a.s.l. elevation. It is bordered to the east and west by the Oriental and Occidental Cordilleras,respectively (Satgé *et al*., 2015). Estimated spatial mean precipitation is 405 mm year^{-1} with a strong north-south gradient (Satgé *et al*., 2019b) and a wet season from October to March (Figure 1d). In terms of land cover, the region is sparsely vegetated with large cultivated areas in the north. The northern and central parts host two important lakes (Lake Titicaca and Poopó) and two big salt pans are located in the southern part of the Altiplano (Uyuni and Coipasa).

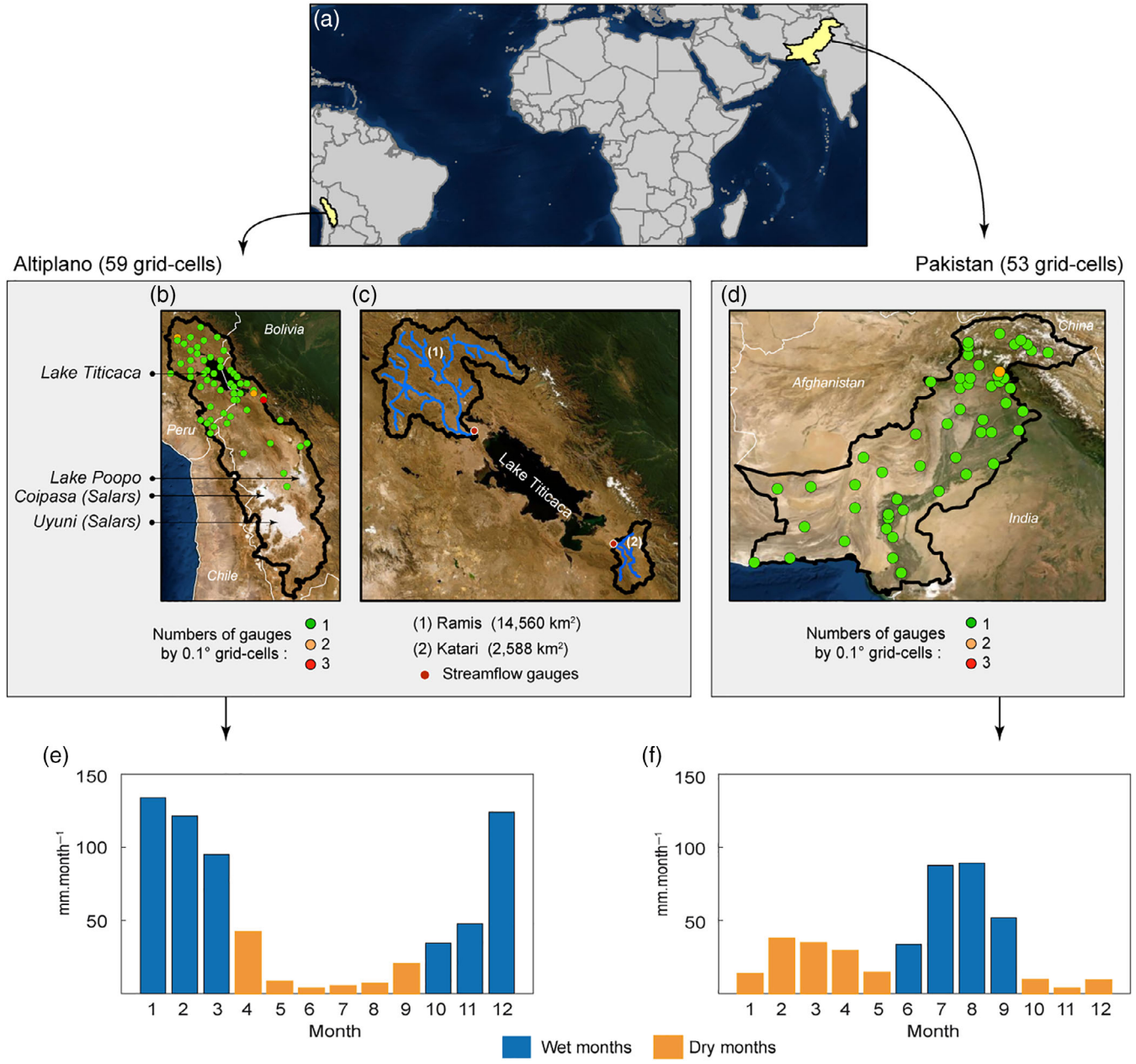

FIGURE 1 Location of the regions of interest across the world (a) with the considered 0.1° grid-cells locations and corresponding gauges number (b,d), considered basins location (c) and mean regional monthly precipitation for the 2007–2015 period based on available gauge observations for the Altiplano (e) and Pakistan (f) [Colour figure can be viewed at wileyonlinelibrary.com]

The second region studied is Pakistan, a country north of the equator with an area of 803,940 km^2. It is divided into four climatic zones from north to south (glacial, humid, arid and extremely arid) (Adnan *et al.*, 2017), with a wet season from June to September (Figure 1e). The glaciated region is located at the northern limit and is mainly covered by glaciers and permanent snow at an average altitude of 4,158 m.a.s.l. The humid region, next to the glacial region, is characterized by the presence of very high mountains of the Hindukush, Karakoram, and Himalaya (HKH) ranges, with mean elevation and precipitation of 1,286 m.a.s.l. and 825 mm year^{-1}, respectively. The central arid region consists in low-lying plains where the main agricultural areas are located, with average altitude and precipitation of 633 m.a.s.l. and 322 mm year^{-1}, respectively. Finally, at the southern boundary towards the Arabian Sea, the extremely arid region receives 133 mm year^{-1} of rain. This barren and bare soil region is located at a mean altitude of 444 m.a.s.l. and includes low, high and dry mountain ranges (Satgé *et al.*, 2018).

2.2 | Datasets

2.2.1 | Hydro-meteorological stations

For the Altiplano region, precipitation data were provided by the Servicio Nacional de Meteorologia e Hidrologia (SENAMHI) for the Bolivian part, while for Peru, data were collected on the Peruvian SENAMHI website. For Pakistan, precipitation data were provided by the Pakistan Meteorological Department (PMD). A total of 126 and 55 rain gauges were made available for the Altiplano and Pakistan, respectively. Only the gauges with more than 80% daily data available for the 2007–2015 period (9 years) were included in the analysis. The records were then aggregated to the 0.1° grid-cell size by averaging the precipitation values of all gauges included in the same 0.1° grid-cell. According to this procedure, 59 and 53 0.1° grid-cells were used as reference in the precipitation estimates for the Altiplano and Pakistan, respectively (Figure 1). Most of the precipitation data come from manned weather stations and are subject to data quality problems. Many of these problems are due to measurement errors by observers, but errors related to instruments and station location are also common. Over the Altiplano, the quality of the gauges has been previously checked (Satgé *et al*., 2016, 2019a) using the Regional Vector Method (RVM) (Espinoza Villar *et al*., 2009). Over Pakistan, the PMD follows the World Meteorological Organization (WMO) standard code WMO–N for the evaluation and correction of gauge-based precipitation data (World Meteorological Organization, 1994).

Streamflow observations records for a seven-year period (2009–2015) were also available at two river basin outlets in the Altiplano (Figure 1): the Katari (2,588 km^2) and the Ramis (14,560 km^2). The basins have an average annual discharge (precipitation) of 52 mm $year^{-1}$ (584 mm .$year^{-1}$) and 160 mm.$year^{-1}$ (733 mm $year^{-1}$), respectively.

2.2.2 | Selected P-datasets

The SM2RAIN algorithm (Brocca *et al*., 2013) estimates precipitation from SM measurements using the inverted soil water balance equation where surface runoff and evapotranspiration rates during the precipitation event were assumed negligible. The SM2RAIN algorithm has been applied (a) to the Climate Change Initiative (CCI) active and passive SM datasets and (b) to SM derived from the Advanced SCATterometer (ASCAT) on board the Meteorological Operational satellites A and B (MetOp-A and -B) to develop the SM2RAIN-CCI (Ciabatta *et al*., 2018) and the SM2RAIN-ASCAT (Brocca *et al*., 2019) daily P-datasets. In addition to the different spatial resolutions, input SM and temporal coverage (Table 1), SM2RAIN-CCI and SM2RAIN-ASCAT differ for the SM2RAIN algorithm calibration. SM2RAIN-ASCAT uses the latest ReAnalysis (ERA5) from the European Centre for Medium-Range Weather Forecasts (ECMWF), while SM2RAIN-CCI uses the Global Precipitation Climatology Centre Full Daily Data (GPCC-FDD) dataset. Due to the different characteristics of the satellite sensors used for creating both the CCI (active and passive) and ASCAT (Metop-A and Metop-B) SM datasets, different calibration periods are taken into account. The SM2RAIN-CCI is calibrated for the 1998–2001, 2002–2006 and 2007–2013 periods, whereas SM2RAIN–ASCAT is calibrated for the 2007–2012 and 2013–2018 periods. Unlike SM2RAIN-CCI, SM2RAIN-ASCAT includes a final climatological correction based on ERA5 to mitigate part of the error coming from SM measurement and retrieval algorithm SM2RAIN. For more information on the SM2RAIN-CCI and -ASCAT P-datasets please refer to Ciabatta *et al*. (2018) and Brocca *et al*. (2019), respectively. The SM2RAIN-CCI and SM2RAIN-ASCAT P-datasets are available online at https://zenodo.org/record/1305021 and https://zenodo.org/record/3405563, respectively.

IMERG is a product of the National Aeronautics and Space Administration (NASA) that uses concepts and components from previous algorithms: TMPA, CMORPH, and PERSIANN. Precipitation estimates from available LEO satellites' PMW sensors are assembled, gridded, intercalibrated and combined with data from GEO IR sensors using the Morphing-Kalman Filter, CMORPH-KF, the Lagrangian time interpolation scheme, and the PERSIANN Cloud Classification System (PERSIANN-CCS). The IMERG P-datasets are currently at version 6 (v.6) and are available at three levels: the early-run (IMERG-E v.6) and late-run (IMERG-L v.6), which are based only on satellite information and the final-run (IMERG-F v.6), which also uses monthly precipitation data from the GPCC to perform a bias correction. For more information, readers are referred to Huffman *et al*. (2019). The IMERG-E, -L and -F v.6 have never been assessed in the Altiplano and Pakistan.

The CHIRPS v.2 precipitation estimates are extracted from the Globally Gridded Satellite (GridSat) and NOAA Climate Prediction Center (CPC) Thermal Infra-Red (TIR) using the Cold Global Duration (CCD) Method (Funk *et al*., 2015). The CCD is first calibrated by using the TRMM Multisatellite Precipitation Analysis (TMPA) and then blended with rain gauge data from different sources and CHPclim dataset. In this process, Coupled Forecast System (CFS) reanalysis precipitation dataset is

TABLE 1 Main characteristics and references of the considered P-datasets

Full name	Acronym	Temporal coverage	Temporal resolution	Spatial coverage	Spatial resolution	References
Soil Moisture to Rain from Advanced SCATerometer	SM2RAIN-ASCAT	2007–present	Daily	Global (land)	12.5 km	Brocca *et al.* (2019)
Soil Moisture to Rain from ESA Climate Change Initiative	SM2RAIN-CCI v.2	1998–2015	Daily	Global (land)	0.25°	Ciabatta *et al.* (2018)
Climate Hazard Group InfraRed Precipitation with Station	CHIRPS v.2	1981–present	Daily	50° (land)	0.05°	Funk *et al.* (2015)
Multi–Source Weighted Ensemble Precipitation v.2.2	MSWEP v.2.2	1979–present	3 hr	Global	0.1°	Beck *et al.* (2019)
IMERG–Early run v.6	IMERG-E v.6	2000–present	30 min	Global	0.1°	Huffman *et al.* (2019)
IMERG–Late run v.6	IMERG-Lv.6	2000–present	30 min	Global	0.1°	Huffman *et al.* (2019)
IMERG–Final run v.6	IMERG-Fv.6	2000–present	30 min	Global	0.1°	Huffman *et al.* (2019)

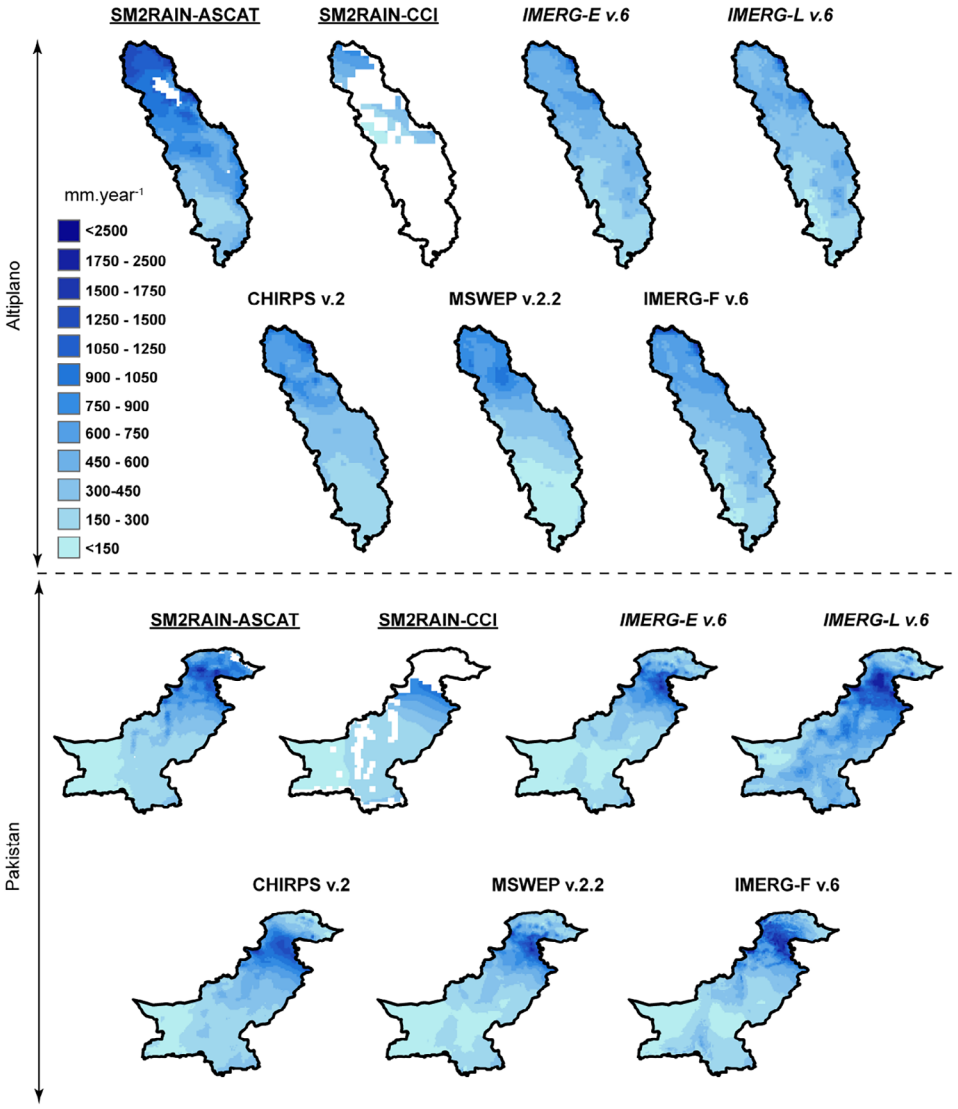

FIGURE 2 Mean annual precipitation maps for the 2007–2015 period retrieved from all P-datasets at 0.1° grid size. For each P-datasets, only the grid cells with more than 80% of available daily data were retained. P-dataset names underlined represent SM2RAIN P-datasets (bottom-up), while regular and italic fonts are used for P-datasets based on 'top-down' approach, independently they may or not may include gauge-based information [Colour figure can be viewed at wileyonlinelibrary.com]

used to fill in the precipitation gaps from the TIR missing observations. For more details, please refer to Funk *et al*. (2015). The data are available at daily time steps at a near global scale coverage (50°N–50°S).

The MSWEP v.2.2 combines precipitation estimates based on satellites (CMORPH, GridSat, GSMaP, TMPA), on reanalysis (ERA-Interim, JRA-55) and on gauges (Worldclim2, GPCC, rain gauges). First, a correlation matrix obtained by comparing satellite-based and reanalysis estimates (previously adjusted with the WorldClim2 database) with observations from rain gauges is used to weight the average of their estimates (Beck *et al*., 2018). Then the resulting precipitation estimates are adjusted with rain gauge data from different sources and the GPCC-FDD dataset. For more information, readers are referred to Beck *et al*. (2019).

Figure 2 shows the mean annual precipitation for the period 2007–2015, derived from the four P-datasets. For the two regions (Altiplano and Pakistan), all P-datasets captured typical north-south precipitation patterns. It is worth mentioning that regions with high uncertainties in CCI SM estimates are removed from the SM2RAIN-CCI v.2 (Ciabatta *et al*., 2018). Therefore, for both the Altiplano and Pakistan, many missing data are observed over glacial regions, frozen soils, complex topography and rainforest areas. In contrast, regions with high uncertainties in ASCAT SM estimates are flagged to ensure data continuity as required in many applications (Brocca *et al*., 2019).

2.2.3 | Comments on the selected P-datasets

Among the selected P-datasets, SM2RAIN-CCI, SM2RAIN-ASCAT, IMERG-E v.6 and IMERG-L v.6 are based solely on satellite information using either 'bottom-up' (SM2RAIN) or 'top-down' approach (IMERG). CHIRPS v.2, MSWEP v.2.2 and IMERG-F v.6 also use a 'top down' concept but include a gauge based dataset for final precipitation adjustment (IMERG-F v.6) or for the recovery of precipitation estimates (CHIRPS v.2, MSWEP v.2.2). Therefore, the selected P-datasets can be separated into three groups:

1 P-datasets based on the 'bottom-up' approach and using only satellite information (SM2RAIN-ASCAT, SM2RAIN-CCI).
2 P-datasets based on the 'top-down' approach and using only satellite information (IMERG-E v.6, IMERG-L v.6)
3 P-datasets based on the 'top-down' approach using both satellite and gauge information (CHIRPS v.2, MSWEP v.2.2 and IMERG-F v.6)

It should be mentioned that precipitation estimates from MSWEP v.2.2, CHIRPS v.2 and IMERG-F v.6 are expected to be more accurate than the non-adjusted P-datasets because some of the gauges data used as a reference are included in these P-datasets.

2.2.4 | GLEAM ETp

To implement the hydrological modelling proposed in this study (see Section 2.2.3), the potential evapotranspiration from the Global Land Evaporation Amsterdam Model version 3 (GLEAM v.3) (ETp) datasets is taken into account (Martens *et al*., 2017). Three GLEAM v.3 ETp datasets are available (a, b and c). These datasets differ in terms of spatial coverage, spatial resolution and forcing data. The GLEAM v.3.a dataset was previously validated in the Altiplano (Satgé *et al*., 2019b) and was therefore selected for this study. GLEAM v.3.a uses the Priestley and Taylor equation to calculate potential evapotranspiration (ETp) using air temperature and net surface radiation from the ERA-Interim reanalysis dataset. GLEAM v.3.a ETp estimates are available for global coverage, with a 0.25° grid and daily time step from 1980 to 2016 (https://www.gleam.eu/).

2.3 | P-Datasets reliability assessment

2.3.1 | P-datasets against gauge observations

SM2RAIN-ASCAT, SM2RAIN-CCI and CHIRPS v.2 P-datasets are only available at daily time steps. The 24-hour period used to accumulate daily rainfall for the P-datasets differs from that used by the reference gauges. This temporal mismatch leads to uncertainties in the conclusions drawn from daily analysis (Satgé *et al*., 2020). For this reason, in this study the assessment is carried out only on a monthly time scale, as was previously done in India (Prakash, 2019). To allow a consistent comparison, all P-datasets were resampled to the 0.1° grid-cell size. The bilinear mean (interpolation) is used for P-datasets at a grid-cell size <0.1° (>0.1°) (Beck *et al*., 2019).

Monthly totals were computed only for months with more than 80% common daily records for all datasets (reference and P-datasets). The accuracy of the monthly P-dataset estimates was assessed using quantitative statistical analysis based on modified Kling–Gupta Efficiency (KGE), an objective function combining correlation (R), bias ($Bias$), and variability ratio (Vr) components (Gupta *et al*., 2009; Kling *et al*., 2012) (Equation 1). We used

KGE because water resource management requires reliable representation of the temporal dynamics of precipitation (measured by R) and volume (measured by *Bias* and *Vr*):

$$\mathrm{KGE}=1-\sqrt{(R-1)^2+(\mathrm{Bias}-1)^2+(Vr-1)^2} \quad (1)$$

where R represents the Pearson coefficient (Equation 2), Bias is the ratio between the mean estimated and observed precipitation (Equation 2) and Vr is the ratio of the estimated and observed coefficients of variation (Equation 3):

$$R=\frac{1}{n}\sum_{1}^{n}\frac{(o_n-\mu_o)*(s_n-\mu_s)}{\sigma_o*\sigma_s}, \quad (2)$$

$$\mathrm{Bias}=\frac{\mu_s}{\mu_o}, \quad (3)$$

$$Vr=\frac{\sigma_s/\mu_s}{\sigma_o/\mu_o}, \quad (4)$$

where μ and σ are the distribution mean and standard deviation, respectively and s and o indicate the estimated and the observed precipitation, respectively. KGE, Bias, Vr and R have their optimum at unity.

The analysis was carried out for the period 2007–2015 considering all the months and the months constituting wet and dry seasons separately (Figure 1d,e).

The values of KGE, *Bias*, R and Vr were computed at each grid-cell location (53 and 59 for the Altiplano and Pakistan, respectively) to assess the P-dataset reliability over space and their median values were used to evaluate it at the regional scale.

In view of the important gaps over space and time for SM2RAIN-CCI v.2 (Figure 2), its performance was assessed on a reduced number of 0.1° grid-cells (14 and 29 for the Altiplano and Pakistan, respectively). To provide a fair comparison of SM2RAIN-CCI reliability with the other P-datasets, the statistical scores are also computed by considering only the available grid-cells for SM2RAIN-CCI.

2.3.2 | P-datasets against streamflow modelling

The sensitivity of streamflow modelling to the P-datasets was assessed at the outlet of two Altiplano basins (Figure 1). The Pakistani basins were not evaluated because most rivers are disturbed by dams that alter streamflow in terms of magnitude and temporal dynamics. The GR4j lumped hydrological model (Perrin *et al*., 2003), which has given good results under various hydro-climatic conditions (e.g., Perrin *et al*., 2003; Coron *et al*., 2012; Grouillet *et al*., 2016; Dakhlaoui *et al*., 2017) particularly in the Andean region (e.g., Hublart *et al*., 2016; Satgé *et al*., 2019a), was chosen to carry out the analysis. The model relies on P and ETp and includes four parameters within specific ranges (Perrin *et al*., 2003). The area-averaged P and ETp values were calculated from the 0.1° grid-cells for each basin using a weighted average for the grid-cells not fully included in the basins. To obtain continuous and spatialized reference precipitation series, the precipitation recorded at the available gauges was previously interpolated using the Inverse Distance Weighted method (IDW) on the 0.1° grid-cell resolution (same as the P-datasets). Streamflow modelling was carried out using as forcing data, each of the P-datasets considered in this study and the P_{ref} (obtained from the gauges) dataset. We used the Modular Assessment of Rainfall–Runoff Models Toolbox v.1.2 (MARRMOT), an open-source modular toolbox for 46 conceptual hydrologic models (Knoben *et al*., 2019a), to run the GR4j hydrological model. For each run, model calibration was based on Nelder–Mead simplex algorithm (Lagarias *et al*., 1998) by optimizing an objective function. KGE (Equation 1) and Nash Shuttle Efficiency score (NSE) (Equation 5) are commonly used as objective functions for calibration of hydrological models (i.e., Jiang and Bauer-Gottwein, 2019; Tarek *et al*., 2019; Fallah *et al*., 2020; Zhang *et al*., 2020). However, KGE and NSE relationship is non-unique (Knoben *et al*., 2019b) so that the P-dataset reliability for the streamflow simulation could differ when using KGE or NSE criteria. In this context, both KGE and NSE are used to avoid any influence of the objective function (Dembélé *et al*., 2020) in the evaluation of the P-dataset reliability. The parameters values are provided in appendice 1.

$$\mathrm{NSE}=\left\{\frac{\sum_{t=1}^{N}\left(Q_{\mathrm{obs}}^{t}-Q_{\mathrm{sim}}^{t}\right)^2}{\left(Q_{\mathrm{obs}}^{t}-\bar{Q}_{\mathrm{sim}}\right)^2}\right\}, \quad (5)$$

where NSE is the Nash–Sutcliffe Efficiency, Q_{obs} and Q_{sim} are, respectively, the observed and simulated streamflow and N is the number of time steps (t) for which observations are available.

The two basins have a seven-year common period (2009–2015) of observed discharge data. For each precipitation input (P_{ref} and P-datasets), the model was calibrated over the 2010–2015 period (6 years) using the 2009 year as a spin-up period. No validation period was chosen because the objective of this study was to assess the sensitivity of the hydrological model to the precipitation input and not to evaluate the robustness of the hydrological model.

3 | RESULTS

3.1 | P-dataset reliability compared with gauge observations at the grid-cells level

Based on KGE, all considered P-datasets (except for SM2RAIN-ASCAT) perform better in the Altiplano than in Pakistan (Figure 3).

In the Altiplano, MSWEP v.2.2 and SM2RAIN-ASCAT have the highest and lowest spatial consistency respectively, as indicated by KGE. However, east of the shore of the Lake Titicaca, MSWEP v.2.2 has the lowest KGE score (Figure 3). For the few available grid-cells, the estimates of SM2RAIN-CCI v.2 are more accurate than those of SM2RAIN-ASCAT as observed north and south of the Lake Titicaca (Figure 4b,c).

In Pakistan, all P-datasets exhibit the lowest KGE values over the northern Himalayan (Figure 3d). In the southern region, MSWEP v.2.2 is the most reliable P-dataset, while CHIRPS v.2, SM2RAIN-ASCAT and -CCI

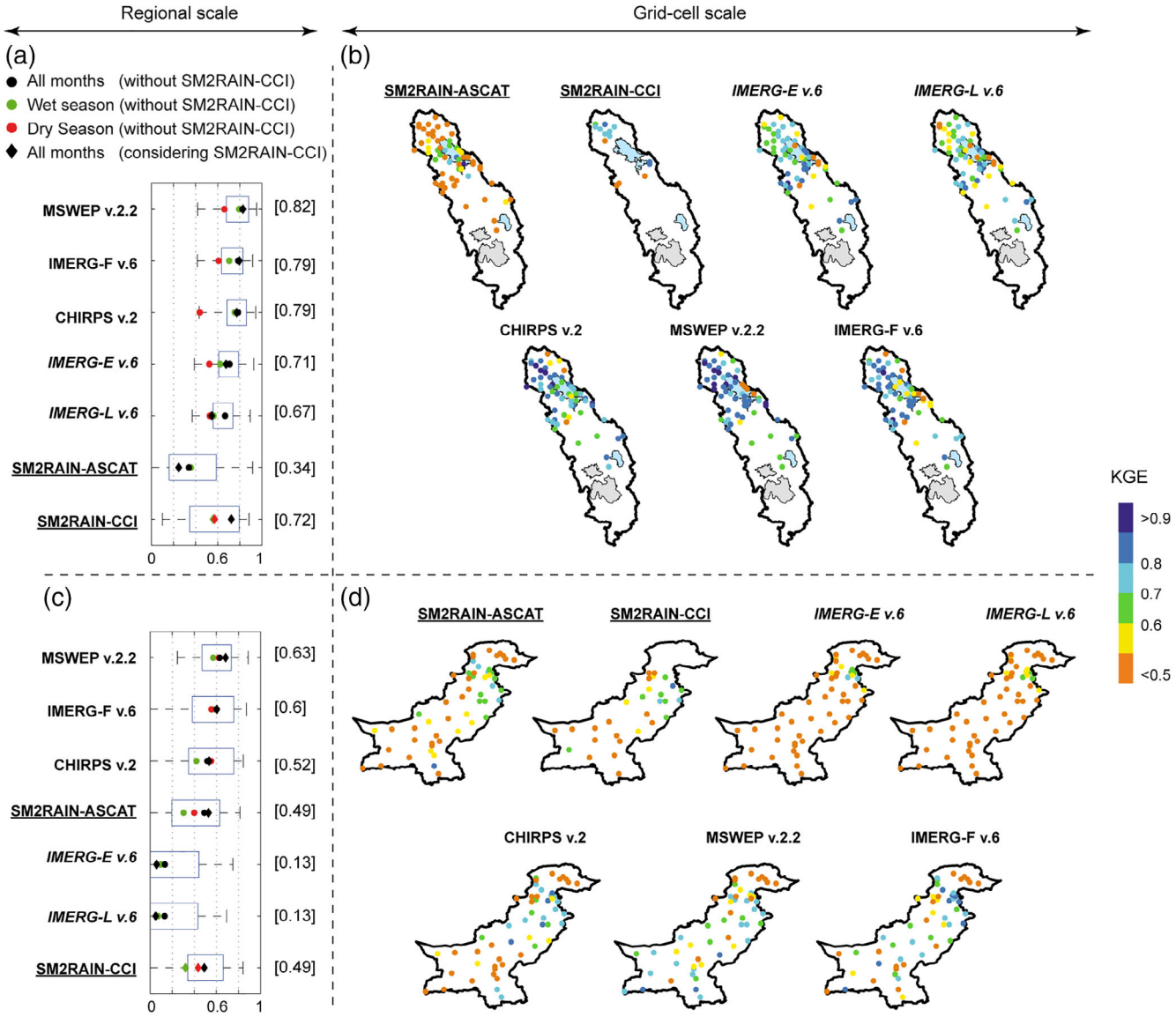

FIGURE 3 P-datasets KGE at the regional and grid-cell level for the Altiplano (a,b) and Pakistan (c,d). In a and c the median KGE values for all considered grid-cells taking wet, dry and all months separately is presented. The right and left edges of the box represent the 25th and 75th percentile values. The P-datasets are sorted from the highest (top) to the lowest (bottom) KGE values. Note that SM2RAIN-CCI v.2 is always placed at the bottom because it is based on a reduced number of 0.1° grid-cells. In b and d, the KGE values at each grid-cell location and considering all months is presented. P-dataset names underlined represent SM2RAIN P-datasets (bottom-up), while regular and italic fonts are used for P-datasets based on 'top-down' approach, independently they may or not may include gauge-based information [Colour figure can be viewed at wileyonlinelibrary.com]

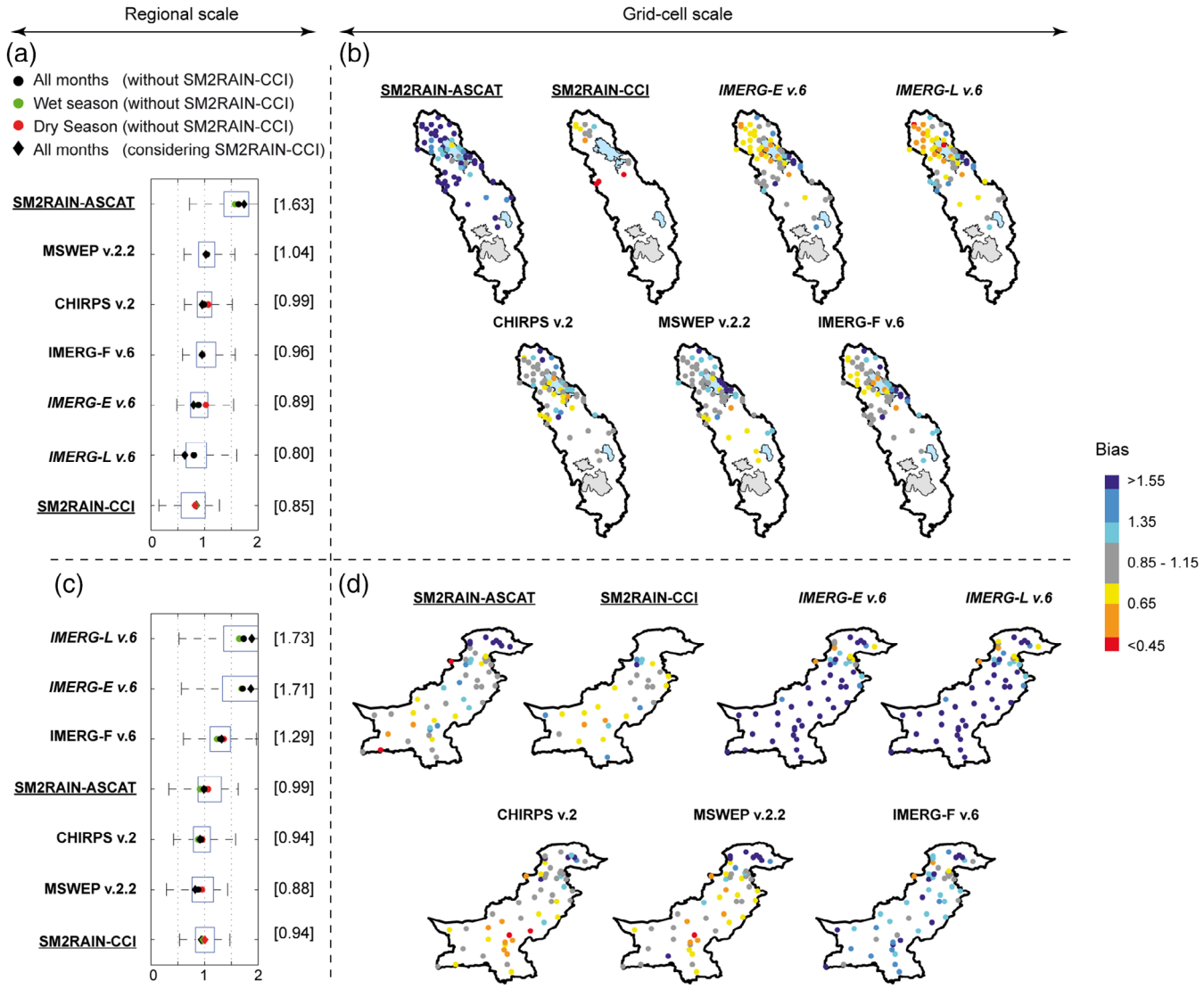

FIGURE 4 Same as Figure 3 but for bias values [Colour figure can be viewed at wileyonlinelibrary.com]

have KGE values lower than 0.5 in most of the considered grid-cells. IMERG-F v.6 has the highest KGE score in the Northeast region.

Interestingly, on a seasonal scale, higher KGE are observed during the wet season (excepting SM2RAIN-CCI) in the Altiplano whereas the converse is true in the case of Pakistan (excepting IMERG-E and -L v.6).

SM2RAIN-ASCAT (-CCI) overestimates (underestimates) monthly precipitation in the Altiplano, with a *Bias* value of 1.63 (0.85). Conversely, in Pakistan SM2RAIN P-datasets *Bias* is small (close to 1), as for CHIRPS v.2, IMERG-F v.6 and MSWEP v.2.2. All versions of IMERG overestimate precipitation in Pakistan. The adjustment based on gauges information slightly reduces the bias on IMERG-F v.6 compared to IMERG-E and -L v.6. The same is observed over the Altiplano, which confirms the positive effect of using gauge-based information. However, for some grid-cells, the precipitation estimates are less biased for the satellite-only versions (IMERG-E v.6, IMERG-L v.6) than for the adjusted versions (IMERG-F v.6). Interestingly, CHIRPS v.2 presents the least biased estimates over the northern region of Pakistan and especially over the Himalayan relief (Figure 4d). Finally, weak seasonal variations are observed for *Bias* in both locations and for all P-datasets (Figure 4a–c).

All considered P-datasets are more correlated with the reference precipitation in the Altiplano than in Pakistan (Figure 5a–c). This is particularly true for SM2RAIN-ASCAT with most of the studied grid-cells having an R value higher (lower) than 0.8 in the Altiplano (Pakistan) (Figure 5b–d). Interestingly IMERG-F v.6 presents high R value in both regions.

Over the Altiplano, MSWEP v.2.2 presents the highest proportion (80%) of grid-cells with $R > 0.9$ followed by SM2RAIN-ASCAT (73%), CHIRPS v.2 (51%), IMERG-F

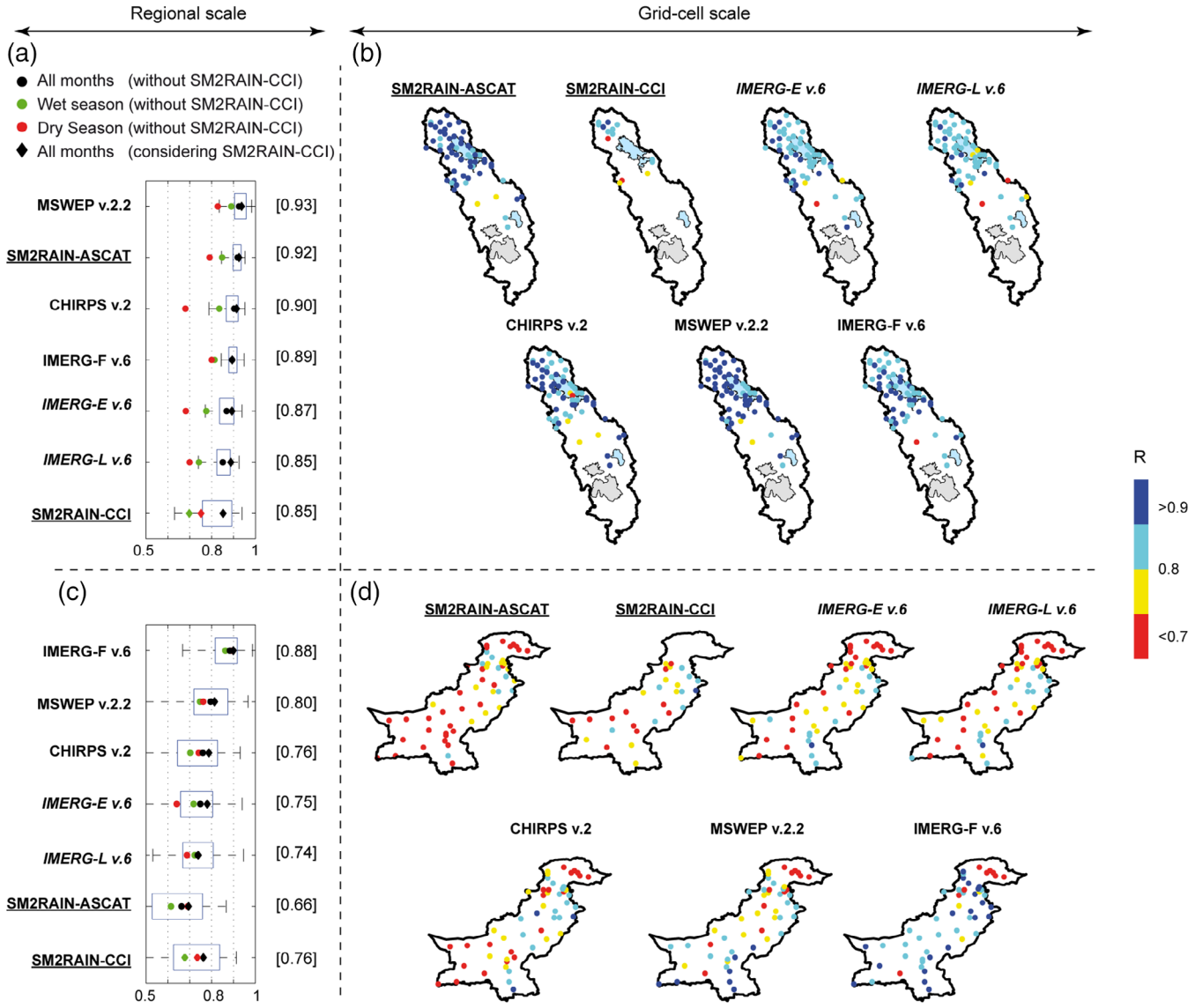

FIGURE 5 Same as Figure 4 but for *R* values [Colour figure can be viewed at wileyonlinelibrary.com]

v.6 (42%), IMERG-E v.6 (25%), IMERG-L v.6 (12%). Over Pakistan, IMERG-F v.6 has the highest proportion (38%) of grid-cells with $R > 0.9$, followed by MSWEP v.2.2 (13%), CHIRPS v.2 (5%), IMERG-E v.6 (2%) and IMERG-L v.6 (2%), while SM2RAIN-ASCAT does not have any grid-cells (Figure 5 d). Across Pakistan, the gauge adjustment clearly improves the *R*-value of IMERG versions (IMERG-E, IMERG-L, IMERG-F v.6).

Interestingly, on a seasonal scale, higher R values are observed during the wet season (excepting SM2RAIN-CCI) in the Altiplano whereas the reverse is true in the case of Pakistan (excepting IMERG-E and -L v.6).

SM2RAIN-ASCAT underestimates the precipitation variability ($Vr < 1$) in both the Altiplano and Pakistan, while SM2RAIN-CCI overestimates (underestimates) the precipitation variability in the Altiplano (Pakistan) (Figure 6 a–c). MSWEP v.2.2 is the most effective in representing the precipitation variability with *Vr* closer to one for the majority of grid-cells (Figure 6b). CHIRPS v.2 and all IMERG v.6 P-datasets have much lower *Vr* values over Pakistan than over the Altiplano (Figure 6 b-d). Finally, *Vr* only has weak seasonal variations in both locations and for all P-datasets (Figure 6 a-c).

3.2 | P-datasets for streamflow modelling

The simulated monthly and daily streamflow obtained using the different P-datasets as forcing data and their associated efficiency scores (KGE, NSE) when compared with the observed streamflow are presented in Figure 7.

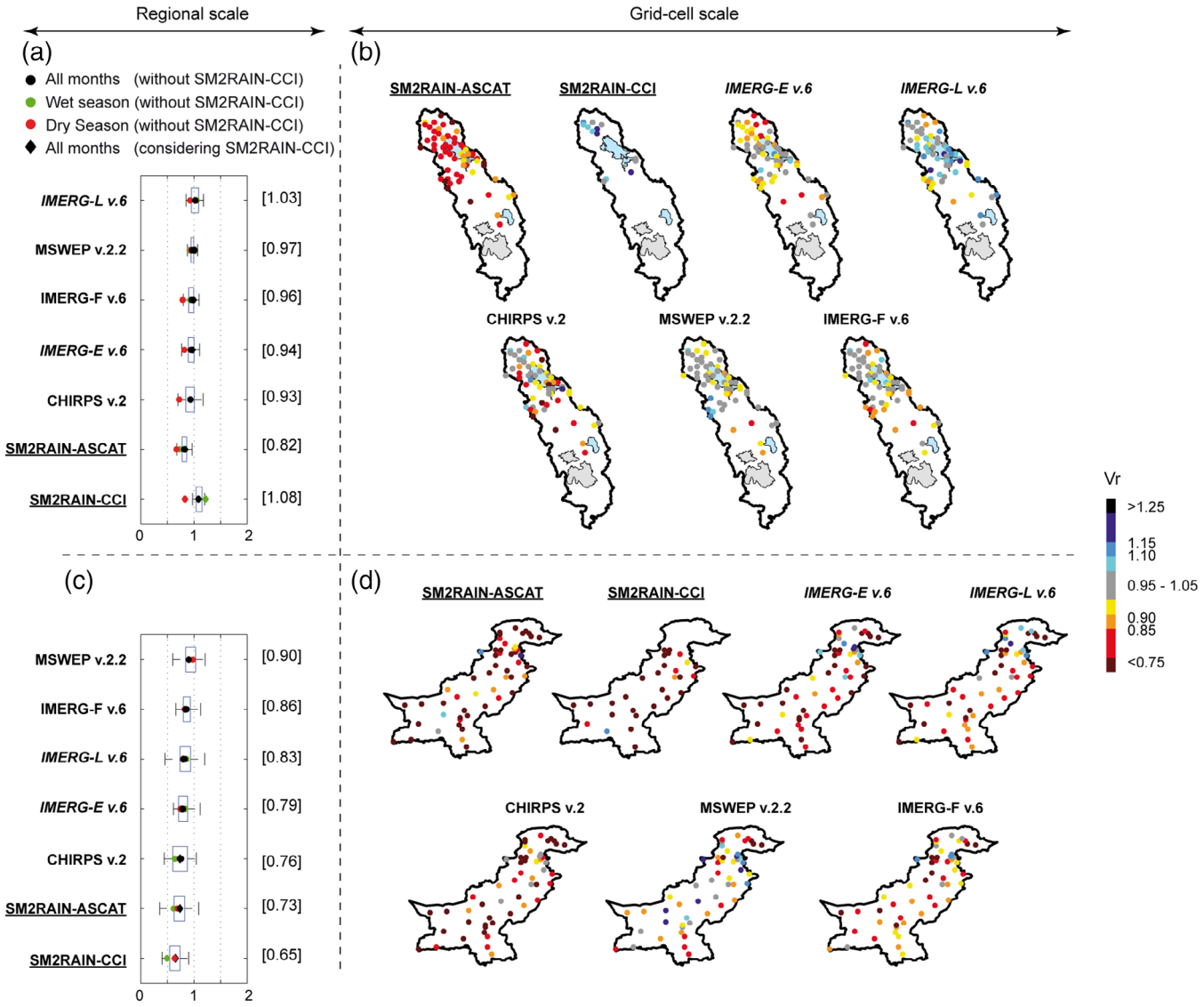

FIGURE 6 Same as Figure 3 but for *Vr* values [Colour figure can be viewed at wileyonlinelibrary.com]

At monthly time steps, the P-dataset consistency for streamflow modelling varies over time. Indeed, some P-datasets over- or underestimate the peak discharge for specific years as observed in the Katari basin for 2010, 2011 and 2014 (Figure 7a). None of the considered P-datasets provide a more accurate streamflow simulation than that obtained with P_{ref} for the Katari (KGE = 0.93) and Ramis (KGE = 0.96) basins. However, the streamflow simulation obtained when using MSWEP v.2.2 or IMERG-F v.6 as forcing data is close to that obtained using P_{ref} as forcing data (KGE > 0.9) with MSWEP v.2.2 (IMERG-F v.6) performing best over the Ramis (Katari) basin. For the Ramis basin, SM2RAIN-ASCAT and SM2RAIN-CCI monthly streamflow simulations are relatively accurate (KGE = 0.9 and 0.89, respectively). For the Katari basin, SM2RAIN-ASCAT has a KGE value equal to 0.9 which is close to those obtained with the P-datasets using gauge-based information (MSWEP v.2.2, CHIRPS v.2 and IMERG-F v.6). SM2RAIN-ASCAT achieves higher KGE scores than satellite-only P-datasets IMERG-E v.6 for both basins and IMERG-L v.6 for the Katari basin.

At daily time steps, the ability of the P-datasets to reproduce the streamflow simulation is higher for the Ramis basin than for the Katari basin (Figure 7e,f). Similarly to monthly time steps, MSWEP v.2.2, CHIRPS v.2 and IMERG-F v.6 achieve the highest KGE scores for both basins, with MSWEP v.2.2 ranking first. Interestingly, the MSWEP v.2.2 streamflow simulation is slightly more reliable than the one using P_{ref} for the Katari basin, and than all other P-datasets for both basins. The latter may be partly due to the inclusion of an adjustment based on daily gauge records compared to IMERG-L v.6 and CHIRPS v.2 which use an

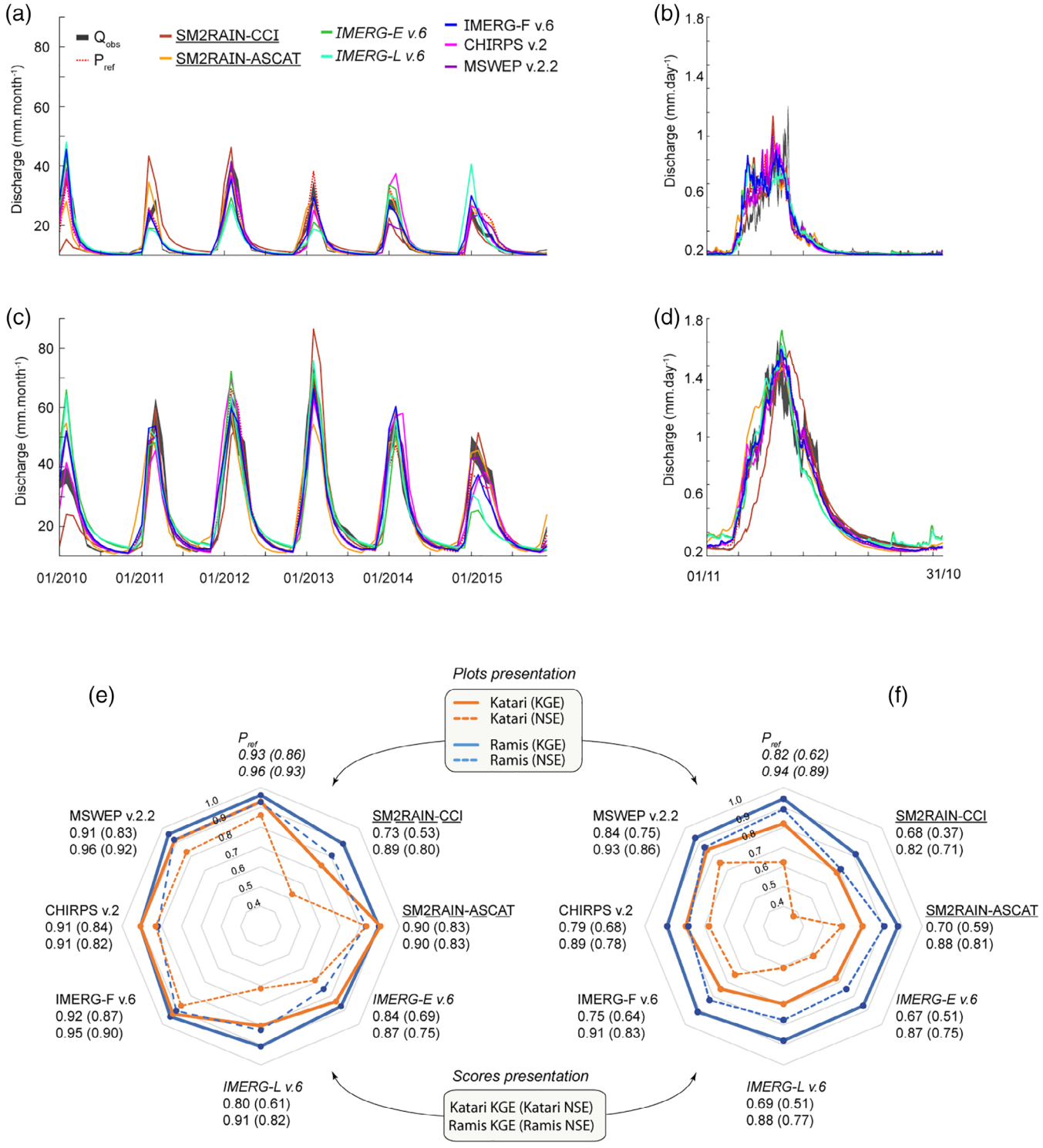

FIGURE 7 Observed versus simulated streamflow using P_{ref} and P-datasets as input data in the hydrological model: monthly streamflow simulation at the Katari (a) and Ramis outlets (c); daily streamflow simulation (represented in the form of mean daily values for the 2010–2015 period to alleviate the figure) at the Katari (b) and Ramis outlets (d); efficiency (KGE and NSE scores) of simulated versus observed streamflow at monthly (e) and daily time step (f). P-dataset names undelined represent SM2RAIN P-datasets (bottom-up), while regular and italic fonts are used for P-datasets based on 'top-down' approach, independently they may or not may include gauge-based information [Colour figure can be viewed at wileyonlinelibrary.com]

adjustment based on monthly gauge ones. SM2RAIN-CCI has the lowest (second lowest) KGE score for the Ramis (Katari) basins while SM2RAIN-ASCAT achieves KGE values similar to higher than the satellite-only based P-datasets IMERG-E and -L v.6 for both basin (Figure 7e).

In spite of the overall lower NSE compared to KGE scores, both indices rank similarly the reliability of the P-datasets for streamflow modelling. Indeed, the P-datasets using gauge information show the best performance for both basins and time scales, with MSWEP v.2.2 and IMERG v.6 performing best. At monthly and daily time scales and for both basins, SM2RAIN-ASCAT shows the closest NSE scores to those obtained with CHIRPS v.2, MSWEP v.2.2 and IMERG-F v.6 and a higher NSE than those obtained with the satellite-only based P-datasets IMERG-E and -L v.6. Therefore, when comparing the P-dataset reliability for streamflow modelling, using KGE or NSE leads to very similar conclusions.

The SM2RAIN-CCI low score (KGE and NSE) for each basin and time step (daily, monthly) is partly attributable to significant gaps in space and time (Figure 2a), which hinder a robust representation of the average precipitation for the two basins.

4 | DISCUSSION

4.1 | P-datasets seasonal consistency

In term of KGE, P-datasets globally perform better during the wet season in the Altiplano, the opposite is observed in Pakistan. In the Altiplano, the monthly precipitation totals are well (badly) distributed between the maximum and minimum values during the wet season (dry season) (Figure 1e). This feature tends to increase the *R* value during the wet season in that region. The converse occurs in Pakistan (Figure 1f) resulting in higher *R* values during the dry season. Similar observations were made in Brazil (Salles *et al*., 2019) and West Africa (Satgé *et al*., 2020) regions. As weak seasonal variations are observed for Bias and Variability ratios in both locations, the KGE value is mainly influenced by the *R* value and follows its seasonal variation (Equation 1).

It is worth to mention that over Pakistan IMERG-E and -L v.6 present a different seasonal variation compared to other P-datasets (higher KGE during the wet season). This could be related to the very high *Bias* value observed for IMERG-E (1.71) and -L (1.73), thus significantly increasing the KGE value. As these P-datasets are less biased during the wet than the dry season (Figure 4c), KGE is higher in the wet season than in the dry season (Figure 3c).

4.2 | P-datasets spatial consistency

At the regional level, P-datasets are more reliable in the Altiplano than in Pakistan, with systematically higher KGE and *R* values (Figures 3 and 4). P-dataset reliability depends on the precipitation retrieval method adopted and its sensitivity to the regional meteorological, topographic and land cover characteristics. From this perspective, Pakistan can be divided into two parts: (a) the southern part comprising arid to extremely arid regions and (b) the northern part entailing the Himalayan mountainous region with permanent snow cover (Adnan *et al*., 2017; Satgé *et al*., 2018). Mountainous regions, snow covered areas and arid context are well known shortcomings in precipitation estimates derived from PMWs and/or IR observations (see for example, Ferraro *et al*., 1998; Levizzani *et al*., 2002; Tian and Peters-Lidard, 2007; Tian *et al*., 2009; Gebregiorgis and Hossain, 2013; Mourre *et al*., 2016). Conversely, the Altiplano consists of a semi-arid and relatively flat region surrounded by mountains (Satgé *et al*., 2015; Satge *et al*., 2016), which is more favourable for PMWs and/or IR precipitation estimates. This fact may partly explain the higher reliability of the 'top-down' based P-datasets (IMERG-E v.6, IMERG-L v.6, IMERG-F v.6, MSWEP v.2.2 and CHIRPS v.2) over the Altiplano than over Pakistan.

Similarly, satellite-based SM estimates are still limited over regions with high topographic complexity, the presence of frozen areas and the occurrence of snowfall (Ciabatta *et al*., 2018; Brocca *et al*., 2019) as observed over northern Pakistan. In addition, significant agricultural activities take place all around the Indus River, which could affect the satellite-based SM signal due to plant cultivation and irrigation practices. It is noteworthy that this drawback is currently used for the detection and quantification of irrigation practices (Brocca *et al*., 2018; Zaussinger *et al*., 2019). The specific Pakistani context reduces the efficiency of satellite-based SM estimates and thus of the SM2RAIN P-datasets (Figure 3).

It is interesting to note that on the Altiplano, SM2RAIN-ASCAT provides the highest *R* value at 32% of the grid-cell locations (Figure 8a,c). This is the case for the grid-cells located on the eastern shore of the Lake Titicaca in the foothills of the oriental cordillera. There, the large variations in land cover (in term of emissivity and surface temperature) and warm cloud precipitation events introduce greater uncertainties in the 'top-down' approach than in the 'bottom-up' approach. This example highlights the complementarity of the 'bottom-up' approach with the 'top-down', as previously reported in different regions (Brocca *et al*., 2016, 2019; Ciabatta *et al*., 2017; Chiaravalloti *et al*., 2018; Massari *et al*., 2019; Zhang *et al*., 2019). Similarly, SM2RAIN-ASCAT has the highest *R* value in the western part of the Altiplano (Figure 8a). Compared to the northern region, the western region is almost isolated from any human footprint that could affect SM (cities, agriculture activities).

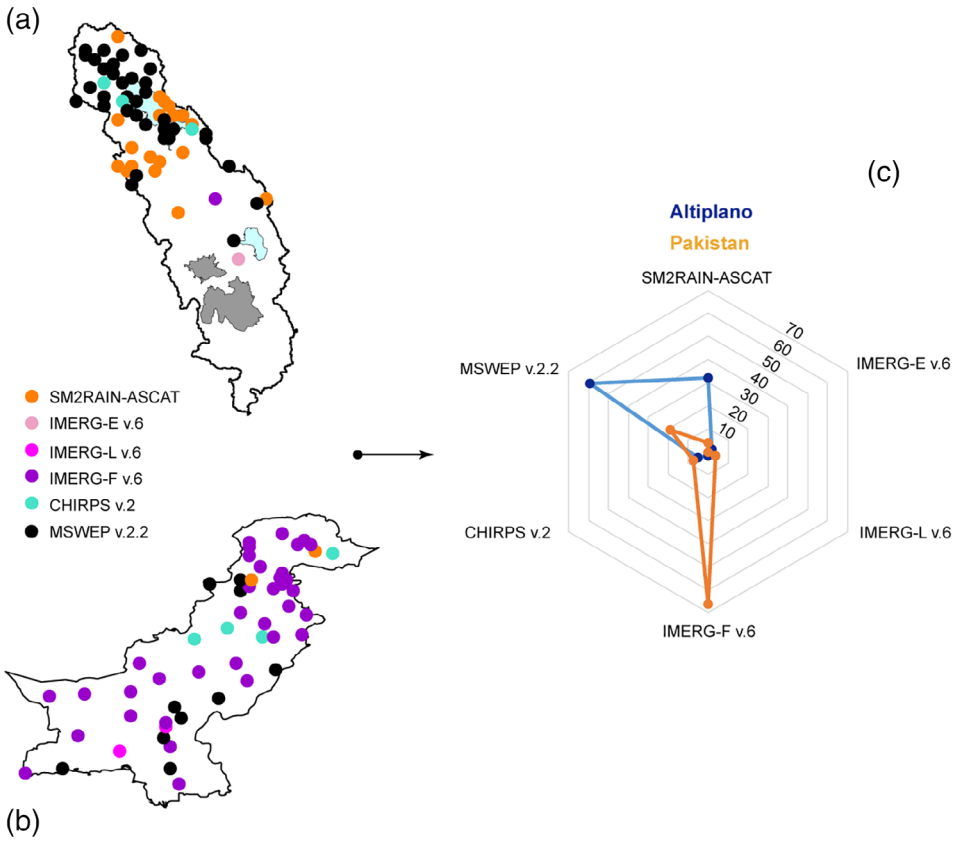

FIGURE 8 Best P-datasets evaluated by R at each considered grid-cell location across the Altiplano (a) and Pakistan (b) with the corresponding number of grid-cells expressed in percent (c) [Colour figure can be viewed at wileyonlinelibrary.com]

Finally, Figure 8 clearly shows that the reliability ranking of P-datasets varies from region to region, with MSWEP v.2.2 and IMERG-F v.6 being performing the best for most grid-cells in the Altiplano (59%) and Pakistan (66%), respectively (Figure 8). Therefore, the results obtained in one region cannot be directly extrapolated to another region and selection of P-datasets should rely on a full reliability assessment. Ideally, different P-datasets are to be used depending on the location where the precipitation estimates are required (Figure 8a,b). In this regard, some studies have already proposed different methods for merging several P-datasets to obtain more reliable precipitation estimates than if a single P-dataset was to be used (i.e., Baez Villanueva et al., 2020; Ehsan Bhuiyan et al., 2019; Muhammad et al., 2018; Rahman et al., 2018).

These studies could be used as guidelines to take advantage of the most reliable P-datasets.

4.3 | Gauges versus streamflow assessment

In order to assess the influence of the indicators used for the P-dataset reliability assessment, the KGE obtained for streamflow simulation is compared with the KGE obtained by comparing average basin precipitation derived from the P-dataset with that obtained with P_{ref} (Figure 9).

On a general way, the P-datasets are better to estimate streamflow than precipitation on a daily or monthly basis (Figure 9). This is consistent with previous results (Satgé *et al.*, 2019a). As precipitation varies spatially, many precipitation events observed at the grid-cell level (areal measurement) may be lost or underestimated at the gauge level (point measurement). Therefore, the P-datasets reliability (based upon a gauge-based evaluation) increases with the number of gauges used to represent the spatial average of the grid-cell measurement (Tang *et al.*, 2018; Salles *et al.*, 2019). In this study, most of the grid-cells have only one gauge, resulting in a 'poor' representation of the areal grid-cell P-datasets estimates. Conversely, the streamflow measurement at the outlet of the basin is 'highly' representative of the basin scale P-dataset estimates. The ability of the indicator used (Rain gauges vs. streamflow gauges) to represent the variable to be assessed (precipitation) influences the evaluation. Therefore, higher KGE are obtained for all P-datasets when using streamflow-based assessment rather than gauge-based assessment (Figure 9).

This difference is more striking for SM2RAIN-ASCAT. Indeed, from gauges-based to streamflow-based assessments, the daily (monthly) KGE value increased from 0.4 to 0.7 (0.53 to 0.9) and from 0.13 to 0.88 (0.23 to 0.90) for the Katari and Ramis basin, respectively. SM2RAIN-ASCAT KGE value obtained for the gauge-

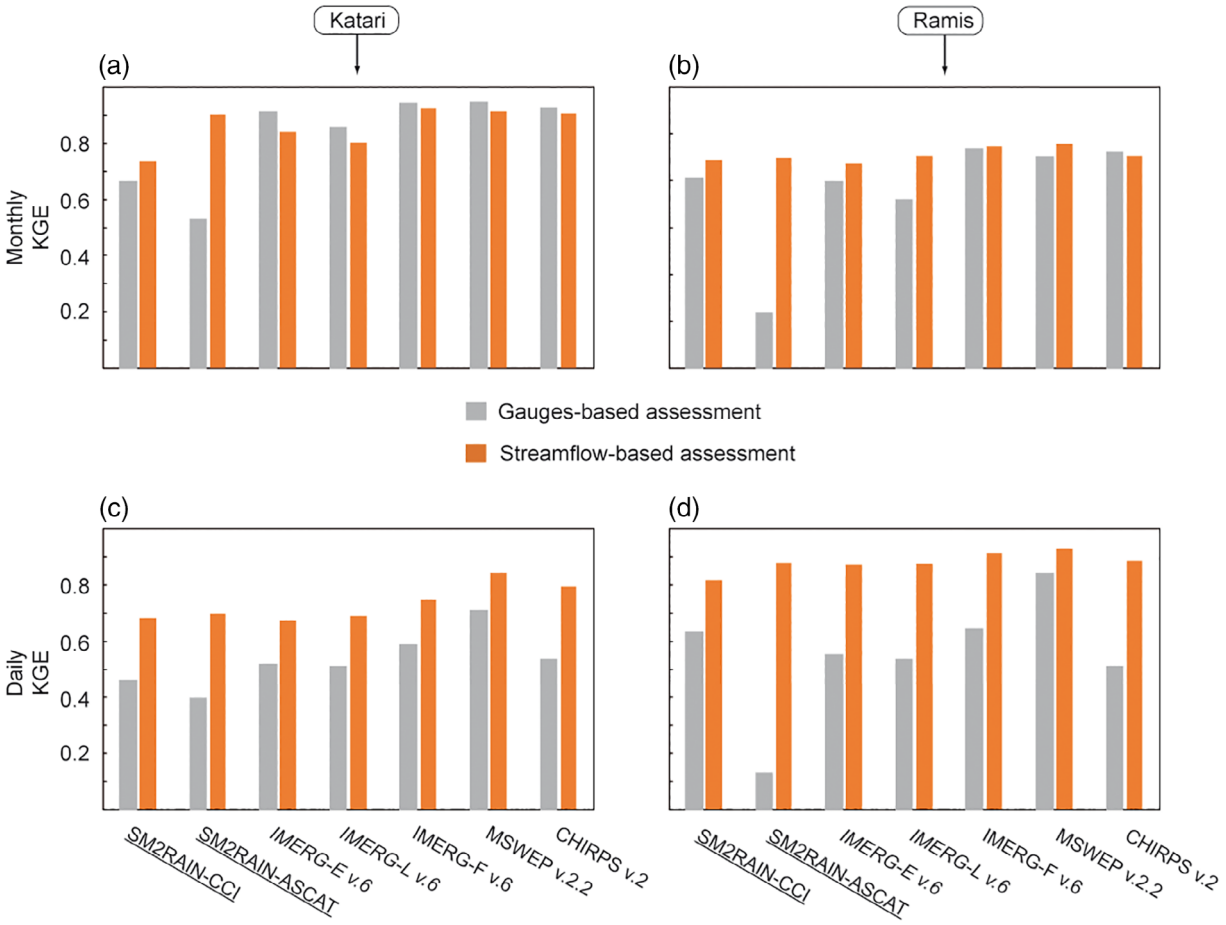

FIGURE 9 KGE value obtained based on the gauges-based and streamflow-based assessment for each basin and at both daily and monthly time step. P-dataset names underlined represent SM2RAIN (bottom-up), while regular and italic fonts are used for 'top-down' approach based P-datasets using or not gauge-based information [Colour figure can be viewed at wileyonlinelibrary.com]

based assessment is particularly low because of the large bias in the precipitation estimates (Figures 3 and 5a). When used as forcing data for streamflow modelling, the P-dataset bias is partially corrected through an optimum hydrological model parameterization. Since the bias has a significant influence on KGE value (Satgé *et al.*, 2020) (Equation 1), its correction increases the KGE. This works as long as the P-dataset describes well the temporal dynamics of the precipitation for the region studied, as measured by the *R* coefficient. Along this line some authors proposed the use of hydrological modelling to adjust P-datasets estimates (i.e., Zhan *et al.*, 2015; Román-Cascón *et al.*, 2017).

5 | CONCLUSIONS

The reliability of newly released SM2RAIN-ASCAT and -CCI P-datasets to reproduce ground-based precipitation records over 2007–2015 and the streamflow records at two basin outlets for the 2010–2015 period were evaluated in the regions of the Altiplano and Pakistan.

Divergent spatial results were obtained. Both SM2RAIN-ASCAT and -CCI replicate the precipitation records in the Altiplano better than in Pakistan. This fact is explained by more favourable meteorological, topographic and land cover characteristics for satellite-based SM estimates in the Altiplano than Pakistan. SM2RAIN-ASCAT and -CCI reliability substantially increases if they are used as forcing data for hydrological models to reproduce streamflow records. This fact comes from (a) the significant bias in the precipitation estimates, which is counterbalanced by the hydrological model parameterization and (b) a better spatial coherence between the P-datasets and the reference (precipitation gauges vs. streamflow gauges).

Despite an important bias, SM2RAIN-ASCAT ability to replicate temporal dynamics of the Altiplano precipitation, evaluated through *R*, is similar that of the well-established state of the art CHIRPS v.2, MSWEP v.2.2 and IMERG-F v.6 P-datasets and even better in some sub regions. Therefore, a suitable bias correction or a specific calibration of SM2RAIN algorithm over the considered regions should considerably increase SM2RAIN-ASCAT

reliability. For instance, the consideration of actual ET into the SM2RAIN algorithm is a good option as it enhances SM2RAIN-ASCAT estimates over areas in which evapotranspiration is important, as shown in the south-western United States and central western Australia (Brocca *et al.*, 2019). Unfortunately, SM2RAIN-CCI has too many gaps in space and time to be used as a reliable precipitation dataset over both the Altiplano and Pakistan.

In an end-user perspective, this study shows that the choice of the best P-datasets must rely on assessments carried out on the target region and involving indicators that take into account the foreseen use of the results.

ORCID

Frédéric Satgé https://orcid.org/0000-0003-3662-6876
Yawar Hussain https://orcid.org/0000-0002-4155-6764

REFERENCES

Adnan, S., Ullah, K., Gao, S., Khosa, A.H. and Wang, Z. (2017) Shifting of agro-climatic zones, their drought vulnerability, and precipitation and temperature trends in Pakistan. *International Journal of Climatology*, 37(February, 529–543. https://doi.org/10.1002/joc.5019.

Ashouri, H., Hsu, K.L., Sorooshian, S., Braithwaite, D.K., Knapp, K. R., Cecil, L.D., Nelson, B.R. and Prat, O.P. (2015) PERSIANN-CDR: daily precipitation climate data record from multisatellite observations for hydrological and climate studies. *Bulletin of the American Meteorological Society*, 96(1), 69–83. https://doi.org/10.1175/BAMS-D-13-00068.1.

Beck, H.E., Pan, M., Roy, T., Weedon, G.P., Pappenberger, F., Van Dijk, A.I.J.M., Huffman, G.J., Adler, R.F. and Wood, E.F. (2019) Daily evaluation of 26 precipitation datasets using Stage-IV gauge-radar data for the CONUS. *Hydrology and Earth System Sciences*, 23, 207–224. https://doi.org/10.5194/hess-23-207-2019.

Beck, H.E., Wood, E.F., Pan, M., Fisher, C.K., Miralles, D.G., Van Dijk, A.I.J.M., McVicar, T.R. and Adler, R.F. (2018) MSWEP V2 global 3-hourly 0.1° precipitation methodology and quantitative assessment. *Bulletin of the American Meteorological Society*, 100, 473–500. https://doi.org/10.1175/BAMS-D-17-0138.1.

Baez-Villanueva, O.M., Zambrano-Bigiarini, M., Beck, H.E., McNamara, I., Ribbe, L., Nauditt, A., Birkel, C., Verbist, K., Giraldo-Osorio, J.D. and Xuan Thinh, N. (2020) RF-MEP: A novel Random Forest method for merging gridded precipitation products and ground-based measurements. *Remote Sensing of Environment*, 239 111606. http://dx.doi.org/10.1016/j.rse.2019.111606.

Brocca, L., Ciabatta, L., Massari, C., Moramarco, T., Hahn, S., Hasenauer, S., Kidd, R., Dorigo, W., Wagner, W. and Levizzani, V. (2014) Soil as a natural rain gauge: Estimating global rainfall from satellite soil moisture data. *Journal of Geophysical Research – Atmospheres*, 119(9), 5128–5141. https://doi.org/10.1002/2014JD021489.

Brocca, L., Filippucci, P., Hahn, S., Ciabatta, L., Massari, C., Camici, S., Bojkov, B. and Wagner, W. (2019) SM2RAIN-ASCAT (2007-2018): global daily satellite rainfall from ASCAT soil moisture. *Earth System Science Data*, 11(4), 1583–1601.

Brocca, L., Massari, C., Ciabatta, L., Moramarco, T., Penna, D., Zuecco, G., Pianezzola, L., Borga, M., Matgen, P. and Martínez-Fernández, J. (2015) Rainfall estimation from in situ soil moisture observations at several sites in Europe: an evaluation of the SM2RAIN algorithm. *Journal of Hydrology and Hydromechanics*, 63(3), 201–209. https://doi.org/10.1515/johh-2015-0016.

Brocca, L., Moramarco, T., Melone, F. and Wagner, W. (2013) A new method for rainfall estimation through soil moisture observations. *Geophysical Research Letters*, 40(5), 853–858. https://doi.org/10.1002/grl.50173.

Brocca, L., Pellarin, T., Crow, W.T., Ciabatta, L., Massari, C., Ryu, D., Su, C.H., Rudiger, C. and Kerr, Y. (2016) Rainfall estimation by inverting SMOS soil moisture estimates: a comparison of different methods over Australia. *Journal of Geophysical Research – Atmospheres*, 121(20), 12,062–12,079. https://doi.org/10.1002/2016JD025382.

Brocca, L., Tarpanelli, A., Filippucci, P., Dorigo, W., Zaussinger, F., Gruber, A. and Fernández-prieto, D. (2018) How much water is used for irrigation ? A new approach exploiting coarse resolution satellite soil moisture products. *International Journal of Applied Earth Observation and Geoinformation*, 73(May, 752–766. https://doi.org/10.1016/j.jag.2018.08.023.

Chiaravalloti, F., Brocca, L., Procopio, A., Massari, C. and Gabriele, S. (2018) Assessment of GPM and SM2RAIN-ASCAT rainfall products over complex terrain in southern Italy. *Atmospheric Research*, 206(February, 64–74. https://doi.org/10.1016/j.atmosres.2018.02.019.

Ciabatta, L., Brocca, L., Massari, C., Moramarco, T., Puca, S., Rinollo, A., Gabellani, S. and Wagne, W. (2015) Integration of satellite soil moisture and rainfall observations over the Italian territory. *American Meteorological Society*, 16, 1341–1355. https://doi.org/10.1175/JHM-D-14-0108.1.

Ciabatta, L., Cinzia, A., Panegrossi, G., Casella, D., Sanò, P., Dietrich, S., Massari, C. and Brocca, L. (2017) Daily precipitation estimation through different microwave sensors: verification study over Italy. *Journal of Hydrology*, 545, 436–450. https://doi.org/10.1016/j.jhydrol.2016.12.057.

Ciabatta, L., Massari, C., Brocca, L., Gruber, A., Reimer, C., Hahn, S., Paulik, C., Dorigo, W., Kidd, R. and Wagner, W. (2018) SM2RAIN-CCI: a new global long-term rainfall data set derived from ESA CCI soil moisture. *Earth System Science Data*, 10, 267–280. https://doi.org/10.5194/essd-10-267-2018.

Coron, L., Andréassian, V., Perrin, C., Lerat, J., Vaze, J., Bourqui, M. and Hendrickx, F. (2012) Crash testing hydrological models in contrasted climate conditions: an experiment on 216 Australian catchments. *Water Resources Research*, 48(5), 1–17. https://doi.org/10.1029/2011WR011721.

Dakhlaoui, H., Ruelland, D., Tramblay, Y. and Bargaoui, Z. (2017) Evaluating the robustness of conceptual rainfall-runoff models under climate variability in northern Tunisia. *Journal of Hydrology*, 550, 201–217. https://doi.org/10.1016/j.jhydrol.2017.04.032.

Dembélé, M., Hrachowitz, M., Savenije, H.H.G., Mariéthoz, G. and Schaefli, B. (2020) Improving the predictive skill of a distributed hydrological model by calibration on spatial patterns with

multiple satellite data sets. *Water Resources Research*, 56(1), 1–26. https://doi.org/10.1029/2019WR026085.

Dinku, T., Ceccato, P., Grover-Kopec, E., Lemma, M., Connor, S.J. and Ropelewski, C.F. (2007) Validation of satellite rainfall products over East Africa's complex topography. *International Journal of Remote Sensing*, 28(7), 1503–1526. https://doi.org/10.1080/01431160600954688.

Dinku, T., Connor, S.J. and Ceccato, P. (2010) In: Gebremichael, M. and Hossain, F. (Eds.) *Satellite Rainfall Applications for Surface Hydrology*. Netherlands, Dordrecht: Springer, pp. 193–204. https://doi.org/10.1007/978-90-481-2915-7.

Espinoza Villar, J.C., Ronchail, J., Guyot, J.L., Cochonneau, G., Naziano, F., Lavado, W., De Olivera, E., Pombosa, R. and Vauchel, P. (2009) Spatio-temporal rainfall variability in the Amazon basin countries (Brasil, Peru, Bolivia, Colombia, and Ecuador). *International Journal of Climatology*, 29, 1574–1594. https://doi.org/10.1002/joc.1791.

Ehsan Bhuiyan, M. A., Nikolopoulos, E. I. and Anagnostou, E. N. (2019) Machine Learning–Based Blending of Satellite and Reanalysis Precipitation Datasets: A Multiregional Tropical Complex Terrain Evaluation. *Journal of Hydrometeorology*, 20 (11), 2147–2161. http://dx.doi.org/10.1175/jhm-d-19-0073.1.

Fallah, A., O, S. and Orth, R. (2020) Climate-dependent propagation of precipitation uncertainty into the water cycle. *Hydrology and Earth System Sciences Discussions*, https://doi.org/10.5194/hess-2019-660. In review, 2020.

Ferraro, R.R., Smith, E.A., Berg, W. and Huffman, G.J. (1998) A screening methodology for passive microwave precipitation retrieval algorithms. *Journal of the Atmospheric Sciences*, 55(9), 1583–1600. https://doi.org/10.1175/1520-0469(1998)055<1583:ASMFPM>2.0.CO;2.

Funk, C., Peterson, P., Landsfeld, M., Pedreros, D., Verdin, J., Shukla, S., Husak, G., Rowland, J., Harrison, L., Hoell, A. and Michaelsen, J. (2015) The climate hazards infrared precipitation with stations—a new environmental record for monitoring extremes. *Scientific Data*, (2), 1–21. https://doi.org/10.1038/sdata.2015.66.

Gebregiorgis, A.S. and Hossain, F. (2013) Understanding the dependence of satellite rainfall uncertainty on topography and climate for hydrologic model simulation. *IEEE Transactions on Geoscience and Remote Sensing*, 51(1), 704–718. https://doi.org/10.1109/TGRS.2012.2196282.

Grouillet, B., Ruelland, D., Ayar, P.V. and Vrac, M. (2016) Sensitivity analysis of runoff modeling to statistical downscaling models in the western Mediterranean. *Hydrology and Earth System Sciences*, 20(3), 1031–1047. https://doi.org/10.5194/hess-20-1031-2016.

Gupta, H.V., Kling, H., Yilmaz, K.K. and Martinez, G.F. (2009) Decomposition of the mean squared error and NSE performance criteria: implications for improving hydrological modelling. *Journal of Hydrology*, 377(1–2), 80–91. https://doi.org/10.1016/j.jhydrol.2009.08.003.

Hussain, Y., Satgé, F., Hussain, M.B., Martinez-Carvajal, H., Bonnet, M.-P., Cárdenas-Soto, M., Roig, H.L. and Akhter, G. (2018) Performance of CMORPH, TMPA, and PERSIANN rainfall datasets over plain, mountainous, and glacial regions of Pakistan. *Theoretical and Applied Climatology*, 131(3-4), 1119–1132. http://dx.doi.org/10.1007/s00704-016-2027-z.

Hirpa, F.a., Gebremichael, M. and Hopson, T. (2010) Evaluation of high-resolution satellite precipitation products over very complex terrain in Ethiopia. *Journal of Applied Meteorology and Climatology*, 49(5), 1044–1051. https://doi.org/10.1175/2009JAMC2298.1.

Hublart, P., Ruelland, D., De Cortazar-Atauri, I.G., Gascoin, S., Lhermitte, S. and Ibacache, A. (2016) Reliability of lumped hydrological modeling in a semi-arid mountainous catchment facing water-use changes. *Hydrology and Earth System Sciences*, 20(9), 3691–3717. https://doi.org/10.5194/hess-20-3691-2016.

Huffman, G. J., Bolvin, D. T., Braithwaite, D., Hsu, K., Joyce, R., Xie, P. and Yoo, S. H. (2019) NASA global precipitation measurement (GPM) integrated multi-satellite retrievals for GPM (IMERG). Algorithm Theoretical Basis Document (ATBD) Version, 6, 26.

Huffman, G. J., Bolvin, D. T. and Nelkin, E. J. (2019b) Integrated Multi-satellitE Retrievals for GPM (IMERG) Technical Documentation. 612(47).

Huffman, G.J., Bolvin, D.T., Nelkin, E.J., Wolff, D.B., Adler, R.F., Gu, G., Hong, Y., Bowman, K.P. and Stocker, E.F. (2007) The TRMM multisatellite precipitation analysis (TMPA): quasi-global, multiyear, combined-sensor precipitation estimates at fine scales. *Journal of Hydrometeorology*, 8(1), 38–55. https://doi.org/10.1175/JHM560.1.

Jiang, L. and Bauer-Gottwein, P. (2019) How do GPM IMERG precipitation estimates perform as hydrological model forcing? Evaluation for 300 catchments across mainland China. *Journal of Hydrology*, 572, 486–500. https://doi.org/10.1016/j.jhydrol.2019.03.042.

Joyce, R.J., Janowiak, J.E., Arkin, P.A. and Xie, P. (2004) CMORPH: a method that produces global precipitation estimates from passive microwave and infrared data at high spatial and temporal resolution. *Journal of Hydrometeorology*, 5(3), 487–503. https://doi.org/10.1175/1525-7541(2004)005<0487:CAMTPG>2.0.CO;2.

Kling, H., Fuchs, M. and Paulin, M. (2012) Runoff conditions in the upper Danube basin under an ensemble of climate change scenarios. *Journal of Hydrology*, 424–425, 264–277. https://doi.org/10.1016/j.jhydrol.2012.01.011.

Kubota, T., Shige, S., Hashizume, H., Aonashi, K., Takahashi, N., Seto, S., Hirose, M., Takayabu, Y.N., Ushio, T., Nakagawa, K., Iwanami, K., Kachi, M. and Okamoto, Ke. (2007) Global Precipitation Map Using Satellite-Borne Microwave Radiometers by the GSMaP Project: Production and Validation. *IEEE Transactions on Geoscience and Remote Sensing*, 45(7), 2259–2275. http://dx.doi.org/10.1109/tgrs.2007.895337.

Knoben, W.J.M., Freer, J.E., Fowler, K.J.A., Peel, M.C. and Woods, R.A. (2019a) Modular assessment of rainfall—runoff models toolbox providing implementations of 46 conceptual hydrologic models as continuous state-space formulations. *Geoscientific Model Development*, 12, 2463–2480. https://doi.org/10.5194/gmd-12-2463-2019.

Knoben, W.J.M., Freer, J.E. and Woods, R.A. (2019b) Technical note: inherent benchmark or not? Comparing Nash-Sutcliffe and Kling-Gupta efficiency scores. *Hydrology and Earth System Sciences*, 23(10), 4323–4331. https://doi.org/10.5194/hess-23-4323-2019.

Koster, R.D., Brocca, L., Crow, W.T., Burgin, M.S. and De Lannoy, J.M. (2016) Precipitation estimation using L-band and

C-band soil moisture retrievals. *Water Resources Research*, 52, 7213–7225. https://doi.org/10.1002/2016WR019024.Received.

Lagarias, J.C., Reeds, J.A., Wright, M.H. and Wright, P.E. (1998) Convergence properties of the nelder–mead simplex method in low dimensions*. *SIAM Journal on Optimization*, 9(1), 112–147. https://doi.org/10.1137/S1052623496303470.

Levizzani, V., Amorati, R. and Meneguzzo, F. (2002). A review of satellite-based rainfall estimation methods., European Commission Project MUSIC Report (EVK1-CT-2000-00058), 66.

Martens, B., Miralles, D.G., Lievens, H., Van Der Schalie, R., De Jeu, R.A.M., Fernández-Prieto, D., Beck, H.E., Dorigo, W.A. and Verhoest, N.E.C. (2017) GLEAM v3: satellite-based land evaporation and root-zone soil moisture. *Geoscientific Model Development*, 10(5), 1903–1925. https://doi.org/10.5194/gmd-10-1903-2017.

Massari, C., Crow, W. and Brocca, L. (2017) An assessment of the accuracy of global rainfall estimates without ground-based observations. *Hydrology and Earth System Sciences*, 21 4347–4361. https://doi.org/10.5194/hess-2017-163.

Massari, C., Maggioni, V., Barbetta, S., Brocca, L., Ciabatta, L., Camici, S., Moramarco, T., Coccia, G. and Todini, E. (2019) Complementing near-real time satellite rainfall products with satellite soil moisture-derived rainfall through a Bayesian inversion approach. *Journal of Hydrology*, 573(March, 341–351. https://doi.org/10.1016/j.jhydrol.2019.03.038.

Mourre, L., Condom, T., Junquas, C., Lebel, T., Sicart, J. E., Figueroa, R. and Cochachin, A. (2016) Spatio-temporal assessment of WRF, TRMM and in situ precipitation data in a tropical mountain environment (Cordillera Blanca, Peru). *Hydrology and Earth System Sciences* 20(1), 125–141. https://doi.org/10.5194/hess-20-125-2016.

Muhammad, W., Yang, H., Lei, H., Muhammad, A. and Yang, D. (2018) Improving the Regional Applicability of Satellite Precipitation Products by Ensemble Algorithm. *Remote Sensing*, 10(4), 577. http://dx.doi.org/10.3390/rs10040577.

Paredes-Trejo, F., Barbosa, H. and dos Santos, C.A.C. (2019) Evaluation of the performance of SM2RAIN-derived rainfall products over Brazil. *Remote Sensing*, 11(9), 1113. https://doi.org/10.3390/rs11091113.

Perrin, C., Michel, C. and Andréassian, V. (2003) Improvement of a parsimonious model for streamflow simulation. *Journal of Hydrology*, 279(1–4), 275–289. https://doi.org/10.1016/S0022-1694(03)00225-7.

Prakash, S. (2019) Performance assessment of CHIRPS, MSWEP, SM2RAIN-CCI, and TMPA precipitation products across India. *Journal of Hydrology*, 571(January, 50–59. https://doi.org/10.1016/j.jhydrol.2019.01.036.

Prakash, S., Sathiyamoorthy, V., Mahesh, C. and Gairola, R.M. (2014) An evaluation of high-resolution multisatellite rainfall products over the Indian monsoon region. *International Journal of Remote Sensing*, 35(9), 3018–3035. https://doi.org/10.1080/01431161.2014.894661.

Rahman, K., Shang, S., Shahid, M. and Li, J. (2018) Developing an Ensemble Precipitation Algorithm from Satellite Products and Its Topographical and Seasonal Evaluations Over Pakistan. *Remote Sensing*, 10(11), 1835. http://dx.doi.org/10.3390/rs10111835.

Rahman, K.U., Shang, S., Shahid, M. and Wen, Y. (2019) Performance assessment of SM2RAIN-CCI and SM2RAIN-ASCAT precipitation products over Pakistan. *Remote Sensing*, 11, 1–24. https://doi.org/10.3390/rs11172040.

Román-Cascón, C., Pellarin, T., Gibon, F., Brocca, L., Cosme, E., Crow, W., Fernández-prieto, D., Kerr, Y.H. and Massari, C. (2017) Correcting satellite-based precipitation products through SMOS soil moisture data assimilation in two land-surface models of di fferent complexity: API and SURFEX. *Remote Sensing of Environment*, 200(April, 295–310. https://doi.org/10.1016/j.rse.2017.08.022.

Salles, L., Satgé, F., Roig, H., Almeida, T., Olivetti, D. and Ferreira, W. (2019) Seasonal effect on spatial and temporal consistency of the new GPM-based IMERG-v5 and GSMaP-v7 satellite precipitation estimates in Brazil's central plateau region. *Water*, 11(4), 668. https://doi.org/10.3390/w11040668.

Satgé, F., Bonnet, M.-P., Gosset, M., Molina, J., Yuque Lima, W., Pillco Zolá, R., Timouk, F. and Garnier, J. (2016) Assessment of satellite rainfall products over the Andean plateau. *Atmospheric Research*, 167, 1–14. https://doi.org/10.1016/j.atmosres.2015.07.012.

Satgé, F., Bonnet, M.P., Timouk, F., Calmant, S., Pillco, R., Molina, J., Lavado-Casimiro, W., Arsen, A., Crétaux, J.F. and Garnier, J. (2015) Accuracy assessment of SRTM v4 and ASTER GDEM v2 over the Altiplano watershed using ICESat/GLAS data. *International Journal of Remote Sensing*, 36(January, 465–488. https://doi.org/10.1080/01431161.2014.999166.

Satgé, F., Defrance, D., Sultan, B., Bonnet, M., Seyler, F., Rouché, N., Pierron, F. and Paturel, J. (2020) Evaluation of 23 gridded precipitation datasets across West Africa. *Journal of Hydrology*, 581, 124412. https://doi.org/10.1016/j.jhydrol.2019.124412.

Satge, F., Denezine, M., Pillco, R., Timouk, F., Pinel, S., Molina, J., Garnier, J., Seyler, F. and Bonnet, M.-P. (2016) Absolute and relative height-pixel accuracy of SRTM-GL1 over the south American Andean plateau. *ISPRS Journal of Photogrammetry and Remote Sensing*, 121, 157–166. https://doi.org/10.1016/j.isprsjprs.2016.09.003.

Satgé, F., Espinoza, R., Zolá, R., Roig, H., Timouk, F., Molina, J., Garnier, J., Calmant, S., Seyler, F. and Bonnet, M.-P. (2017b) Role of climate variability and human activity on Poopó Lake droughts between 1990 and 2015 assessed using remote sensing data. *Remote Sensing*, 9(3), 218. https://doi.org/10.3390/rs9030218.

Satgé, F., Hussain, Y., Bonnet, M.-P., Hussain, B., Martinez-Carvajal, H., Akhter, G. and Uagoda, R. (2018) Benefits of the successive GPM based satellite precipitation estimates IMERG–V03, –V04, –V05 and GSMaP–V06, –V07 over diverse geomorphic and meteorological regions of Pakistan. *Remote Sensing*, 10(9), 1373. https://doi.org/10.3390/rs10091373.

Satgé, F., Hussain, Y., Xavier, A., Pillco, R., Salles, L., Timouk, F., Seyler, F., Garnier, J., Frappart, F. and Bonnet, M. (2019b) Unraveling the impacts of droughts and agricultural intensification on the Altiplano water resources. *Agricultural and Forest Meteorology*, 279(April, 107710. https://doi.org/10.1016/j.agrformet.2019.107710.

Satgé, F., Ruelland, D., Bonnet, M., Molina, J. and Pillco, R. (2019a) Consistency of satellite-based precipitation products in space and over time compared with gauge observations and snow-hydrological modelling in the Lake Titicaca region. *Hydrology and Earth System Sciences*, 23, 595–619. https://doi.org/10.5194/hess-23-595-2019.

Satgé, F., Xavier, A., Zolá, R., Hussain, Y., Timouk, F., Garnier, J. and Bonnet, M.-P. (2017a) Comparative assessments of the latest GPM Mission's spatially enhanced satellite rainfall products over the Main Bolivian watersheds. *Remote Sensing*, 9(4), 369. https://doi.org/10.3390/rs9040369.

Sharifi, E., Eitzinger, J. and Dorigo, W. (2019) Performance of the state-of-the-art gridded precipitation products over mountainous terrain: a regional study over Austria. *Remote Sensing*, 11 (17), 1–20. https://doi.org/10.3390/rs11172018.

Shen, Y., Xiong, A., Wang, Y. and Xie, P. (2010) Performance of high-resolution satellite precipitation products over China. *Journal of Geophysical Research*, 115(D2), D02114. https://doi.org/10.1029/2009JD012097.

Sorooshian, S., Hsu, K.-L., Gao, X., Gupta, H.V., Imam, B. and Braithwaite, D. (2000) Evaluation of PERSIANN system satellite–based estimates of tropical rainfall. *Bulletin of the American Meteorological Society*, 81(9), 2035–2046. https://doi.org/10.1175/1520-0477(2000)081<2035:EOPSSE>2.3.CO;2.

Souto, J., Beltrao, N. and Teodoro, A. (2019) Performance of remotely sensed soil moisture for temporal and spatial analysis of rainfall over São Francisco River basin, Brazil. *Geosciences*, 9(3), 144. https://doi.org/10.3390/geosciences9030144.

Tang, G., Behrangi, A., Long, D., Li, C. and Hong, Y. (2018) Accounting for spatiotemporal errors of gauges: a critical step to evaluate gridded precipitation products. *Journal of Hydrology*, 559, 294–306. https://doi.org/10.1016/j.jhydrol.2018.02.057.

Tarek, M., Brissette, F. and Arsenault, R. (2019) Evaluation of the ERA5 reanalysis as a potential reference dataset for hydrological modeling over North-America. *Hydrology and Earth System Sciences*, 24, 2527–2544. https://doi.org/10.5194/hess-2019-316.

Tarpanelli, A., Massari, C., Ciabatta, L., Filippucci, P., Amarnath, G. and Brocca, L. (2017) Advances in water resources exploiting a constellation of satellite soil moisture sensors for accurate rainfall estimation. *Advances in Water Resources*, 108, 249–255. https://doi.org/10.1016/j.advwatres.2017.08.010.

Tian, Y. and Peters-Lidard, C.D. (2007) Systematic anomalies over inland water bodies in satellite-based precipitation estimates. *Geophysical Research Letters*, 34(14), L14403. https://doi.org/10.1029/2007GL030787.

Tian, Y., Peters-Lidard, C.D., Eylander, J.B., Joyce, R.J., Huffman, G.J., Adler, R.F., Hsu, K.-L., Turk, F.J., Garcia, M. and Zeng, J. (2009) Component analysis of errors in satellite-based precipitation estimates. *Journal of Geophysical Research*, 114(D24), D24101. https://doi.org/10.1029/2009JD011949.

World Meteorological Organization *Guide to Hydrological Practices: Data Acquisition and Processing, Analysis, Forecasting and Other Applications*, 1994.

Yamamoto, M.K. and Shige, S. (2014) Implementation of an orographic/nonorographic rainfall classification scheme in the GSMaP algorithm for microwave radiometers. *Atmospheric Research*, 163, 36–47. https://doi.org/10.1016/j.atmosres.2014.07.024.

Zaussinger, F., Dorigo, W., Gruber, A., Tarpanelli, A., Filippucci, P. and Brocca, L. (2019) Estimating irrigation water use over the contiguous United States by combining satellite and reanalysis soil moisture data. *Hydrology and Earth System Sciences*, 23, 897–923.

Zhan, W., Pan, M., Wanders, N. and Wood, E.F. (2015) Correction of real-time satellite precipitation with satellite soil moisture observations. *Hydrology and Earth System Sciences*, 19, 4275–4291. https://doi.org/10.5194/hess-19-4275-2015.

Zhang, L., Li, X., Cao, Y., Nan, Z., Wang, W., Ge, Y., Wang, P. and Yu, W. (2019) Evaluation and integration of the top-down and bottom-up satellite precipitation products over mainland China evaluation and integration of the top-down and bottom-up satellite precipitation products over mainland China. *Journal of Hydrology*, 581, 124456. https://doi.org/10.1016/j.jhydrol.2019.124456.

Zhang, L., Ren, D., Nan, Z., Wang, W., Zhao, Y., Zhao, Y., Ma, Q. and Wu, X. (2020) Interpolated or satellite-based precipitation? Implications for hydrological modeling in a meso-scale mountainous watershed on the Qinghai-Tibet plateau. *Journal of Hydrology*, 583, 124629. https://doi.org/10.1016/j.jhydrol.2020.124629.

SUPPORTING INFORMATION

Additional supporting information may be found online in the Supporting Information section at the end of this article.

How to cite this article: Satgé F, Hussain Y, Molina-Carpio J, *et al.* Reliability of SM2RAIN precipitation datasets in comparison to gauge observations and hydrological modelling over arid regions. *Int J Climatol*. 2020;1–20. https://doi.org/10.1002/joc.6704